

# **Design, Synthesis and Biological Characterization of Histone Deacetylase 8 (HDAC8) Proteolysis Targeting Chimeras (PROTACs) with Anti-Neuroblastoma Activity**

*Salma Darwish<sup>1,2</sup>, Ehab Ghazy<sup>1,2</sup>, Tino Heimburg<sup>1</sup>, Daniel Herp<sup>3</sup>, Patrik Zeyen<sup>1</sup>,  
Johannes Ridinger<sup>4,5,6</sup>, Karin Schmidtkunz<sup>3</sup>, Dina Robaa<sup>1</sup>, Frank Erdmann<sup>1</sup>, Matthias  
Schmidt<sup>1</sup>, Christophe Romier<sup>7</sup>, Manfred Jung<sup>3</sup>, Ina Oehme<sup>4,5,6</sup>, Wolfgang Sippl<sup>1\*</sup>*

<sup>1</sup> *Department of Medicinal Chemistry, Institute of Pharmacy, Martin-Luther University of  
Halle-Wittenberg, 06120 Halle/Saale, Germany*

<sup>2</sup> *Department of Pharmaceutical Chemistry, Faculty of Pharmacy, Alexandria University,  
21521 Alexandria, Egypt*

<sup>3</sup> *Institute of Pharmaceutical Sciences, University of Freiburg, 79104 Freiburg, Germany*

<sup>4</sup> *Hopp Children's Cancer Center Heidelberg (KITZ), Im Neuenheimer Feld 280, 69120  
Heidelberg, Germany*

<sup>5</sup> *Clinical Cooperation Unit Pediatric Oncology, German Cancer Research Center (DKFZ), Im  
Neuenheimer Feld 280, 69120 Heidelberg, Germany*

<sup>6</sup> *German Cancer Consortium (DKTK), Im Neuenheimer Feld 280, 69120 Heidelberg,  
Germany*

<sup>7</sup> *Université de Strasbourg, CNRS, INSERM, Institut de Génétique et de Biologie Moléculaire  
et Cellulaire (IGBMC), Département de Biologie Structurale Intégrative, 67404 Illkirch Cedex,  
France*

\*corresponding author email : [wolfgang.sippl@pharmazie.uni-halle.de](mailto:wolfgang.sippl@pharmazie.uni-halle.de)

## **Abstract**

While histone deacetylases (HDACs) are known as modulators of epigenetic gene regulation, they also control the activity of non-histone protein substrates. The isozyme HDAC8 plays a role in inhibiting apoptosis and increasing cancer cell proliferation. As a result, HDAC8 is considered a potential target in the treatment of cancer forms such as T-cell lymphoma, gastric adenocarcinoma, hepatocellular carcinoma, and childhood neuroblastoma. The present work describes the development of proteolysis targeting chimera (PROTAC) of HDAC8 based on substituted benzhydroxamic acids previously reported as potent and selective HDAC8 inhibitors. Within this study, we have developed the first in class HDAC8 selective PROTAC and investigated the effect on protein degradation and on the proliferation of neuroblastoma cells. The combination of structure-guided synthesis, *in vitro* screening and cellular testing resulted in cereblon (CRBN) based HDAC8 PROTACs that showed anti-neuroblastoma activity in cells.

*Keywords: histone deacetylases (HDAC), HDAC8, proteolysis targeting chimera (PROTAC), CRBN, neuroblastoma, synthesis*

### **I. Introduction:**

Epigenetic processes include among others DNA methylation and post-translational modifications of histone tails. These marks influence gene expression through regulating the DNA readiness for the binding of the RNA polymerase and the transcription factors. Acetylation or acylation of the lysine residues of the histone tail are post-translational modifications that result in the relaxation of the chromatin through reduction of the interaction between histone and DNA. Enzymes that are responsible for this acyl mark introduction are known as histone acetyltransferases

(HATs). The removal of acetyl/acyl marks take place by the so-called histone deacetylases (HDACs). Both opposing chromatin-modifying enzymes additionally target non-histone proteins, e.g. tubulin in case of HDAC6 and SMC3 in case of HDAC8 [1-6].

Eukaryotic histone deacetylases are grouped based on their sequence homology into four classes. While class I (HDAC1, 2, 3, and 8), II (IIa: HDAC4, 5, 7, and 9; IIb: HDAC6 and 10) and IV (HDAC11) members show a zinc-dependent catalytic mechanism, members of class III (Sirt1-7) use NAD<sup>+</sup> cofactor to carry out deacylation. Other modifications involving individual HDACs are demalonylation, desuccinylation and decrotonylation [7-10].

Abnormal acetylation/acylation of histones and non-histone proteins has been found to contribute to the development of various diseases including cancers of different organs such as lung, breast, and liver along with lymphoma and neuroblastoma [6,4,11,12].

HDAC8 is a unique class I zinc-dependant HDAC that plays a role in the invasion and metastasis of cancer [13]. Its upregulation inhibits apoptosis and increases cancer cell proliferation. As a result, it is considered a potential target in the treatment of many cancers such as T-cell lymphoma, gastric adenocarcinoma, hepatocellular carcinoma, and childhood neuroblastoma [11,14-17].

Neuroblastoma is the most common childhood extracranial solid tumour. It emerges from precursor cells in the sympathetic nervous system leading to the development of tumours in the adrenal glands and/or the sympathetic ganglia. According to the stage of the disease, age of the patient and genetic mutations, patients are classified into low, intermediate, and high-risk groups. There is also a special group of metastatic

neuroblastoma, namely the 4S group, that is characterised by increased spontaneous incidence of regression and high survival rate despite metastasis into liver, skin and bone marrow [18,19].

From all classical HDACs (class I, II and IV), only HDAC8 expression could be significantly correlated with the advanced stage of the disease and metastasis. In 4S neuroblastoma cases, HDAC8 was found to be downregulated. Also, inhibition of proliferation, and induction of cell cycle arrest and differentiation such as the outgrowth of neurite-like structures was achieved in cultured neuroblastoma cells by the knockdown of HDAC8 [20,21]. Thereby selective HDAC8 inhibition is considered a very promising strategy in neuroblastoma therapy. However, so far, compounds selectively targeting HDAC8 are characterized by low in vivo stability [21].

Due to the potential therapeutic effect of HDAC8 inhibition in multiple diseases especially cancer, there is great interest in developing selective HDAC8 inhibitors [11,12]. The inhibitory activity of HDAC inhibitors designed to act on class I, II and IV members, is mediated through the interaction of the inhibitor with the zinc ion in the catalytic site through a zinc binding group (ZBG). Besides the ZBG, the inhibitors' pharmacophore is generally composed of a linker mimicking the lysine chain and a cap group which interacts with the protein and affects the isoform selectivity [7].

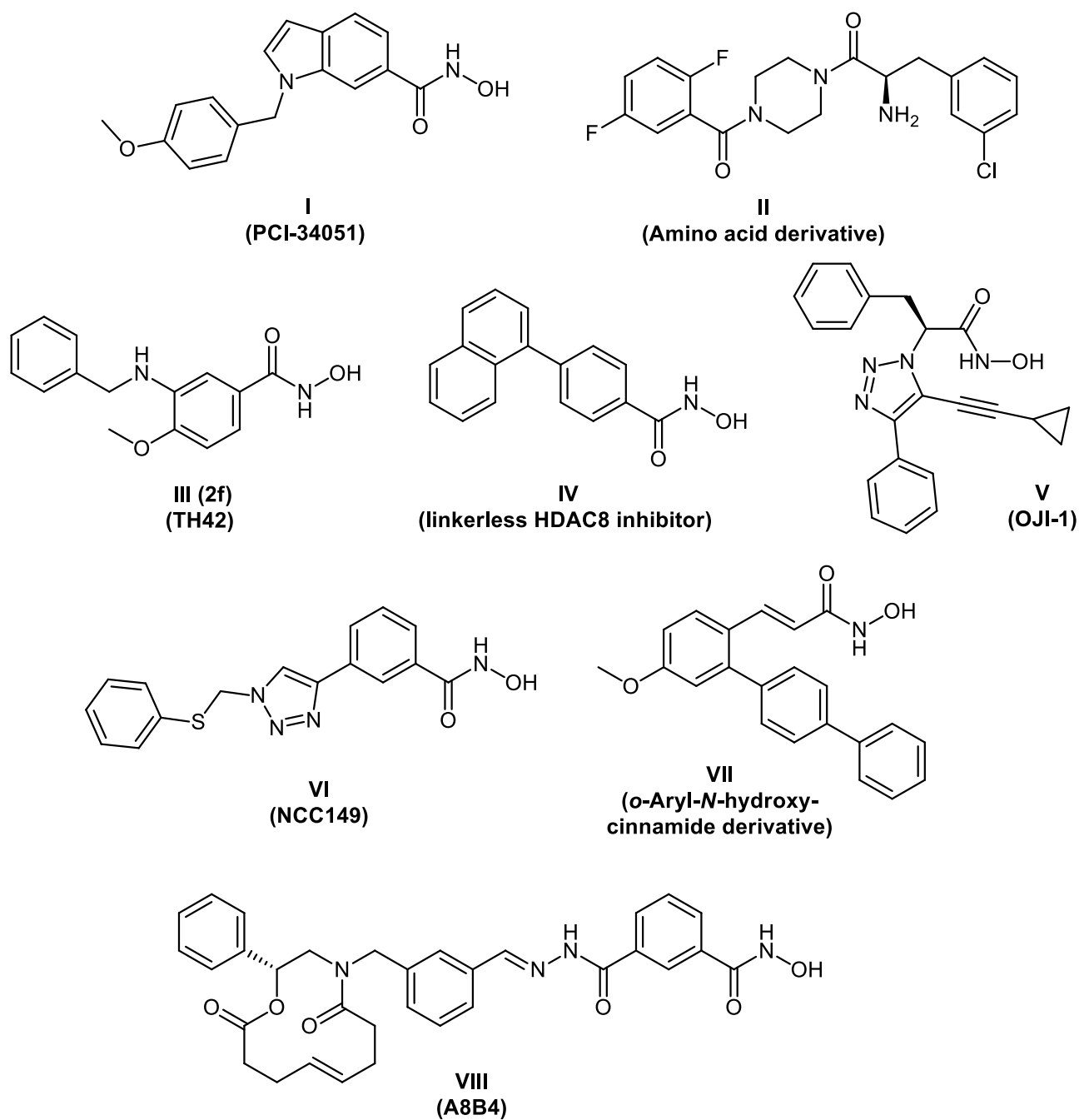


**Figure 1.** Chemical structures of reported HDAC8 inhibitors.

In recent years, several HDAC8 inhibitors have been reported (representative examples in Fig. 1.) [14,22-30]. In 2008, PCI-34051 **I** was reported as a potent and selective HDAC8 inhibitor. It shows good selectivity *in vitro* for HDAC8 compared to other subtypes tested (HDACs 1, 2, 3, 6 and 10) [14]. As reported by Zhao et al., targeted inhibition of HDAC8 using **I** was found to increase the doxorubicin sensitivity

of neuroblastoma cells through miR-137 upregulation and MDR1 suppression leading to the suppression of the cancer cells' growth [28].

Chemotypes other than hydroxamic acids have also been reported to potently inhibit HDAC8. In the investigation made by Whitehead et al., the amino acid derivative **II** showed good activity against HDAC8 with an  $IC_{50}$  of 0.20  $\mu$ M. It also exhibited a good selectivity profile against HDAC1, HDAC2 and HDAC6 [29].

In 2017, we reported the synthesis of a series of para-substituted 3-aminobenzhydroxamic acids as potent HDAC8 inhibitors. Compound **III** with a methoxy group in the para position exhibited strong HDAC8 inhibitory activity ( $IC_{50}$  = 0.07  $\mu$ M) coupled with selectivity over both HDAC isoforms 1 and 6 [30]. In addition, compound **III** showed anti-proliferative effect in several neuroblastoma cell lines.

The aforementioned HDAC8 inhibitors were designed based on the occupancy pharmacology in which the inhibitor exerts its function only by occupying the active site instead of the biological substrate. Among the advantages of protein degraders is their special pharmacology that allows them to target scaffolding proteins without enzymatic functions and to regulate the level of the targeted protein [31]. As stated by Crews and Lai [32] protein degraders can be divided into three classes namely, selective hormone receptor degraders, hydrophobic tagging and proteolysis-targeting chimeras (PROTACs).

The concept of hydrophobic tagged protein degraders (HyT) is based on the addition of a hydrophobic moiety such as adamantane to a known ligand of the targeted protein, forming bifunctional molecules. Till now, the exact mechanism of action is not fully understood and there are at least two possible modes of action. The first proposed mode of action is that the hydrophobic tag destabilizes the protein of

interest (POI), thereby recruiting endogenous chaperones and inducing POI proteasomal degradation. An alternative hypothesis is that chaperones recognize the hydrophobic tag directly and mark the protein for degradation [32-34].

Since its first report in 2001 by Sakamoto et al. [35] PROTAC technology has drawn a lot of attention over the last years. To date, this technology has been used to target various groups of proteins including those still referred to as undruggable according to the occupancy-driven pharmacology. PROTACs are heterobifunctional molecules whose mode of action is based on mimicking the physiological protein degradation system, namely the ubiquitin proteasome system (UPS). The PROTAC molecule is composed of two functionalities attached by a linker. One moiety binds to the POI while the other binds to an E3 ligase, as the degradation machinery recruiting unit, to form a ternary complex which results in the ubiquitination followed by elimination of the targeted protein by the proteasomes leading to its degradation [31-33,36].

In case the interaction of the small molecule-based PROTAC with the POI is non-covalent, the ternary complex dissociates and the PROTAC molecule can bind to another target molecule. As a result of the catalytic PROTAC activity sub-stoichiometric amounts can be applied leading to the minimization of the off-targets effects [31,33]. Another benefit of PROTACs is the enhancement of selectivity towards the POI. It has been proven that induced protein-protein interaction between the POI and the E3 ligase, is necessary for the cooperative formation of the ternary complex required for selective degradation to take place. Consequently, many selective degraders could be developed using ligands that are unselective towards the POI [36-38]. Another advantage of this technology is the longer duration of action in comparison to the conventional inhibitors, as regaining of the activity requires the de novo synthesis of the protein [32].

In the past few years, large interest to target HDACs using the PROTAC technology developed. In 2018, Schiedel et al. published the development of the first degrader of an epigenetic eraser protein which was a Sirt2 selective PROTAC [39]. In the same year, Yang et al. were able to synthesize the first HDAC6 PROTAC utilizing a non-selective HDAC-inhibitor. This was linked to the cereblon E3 ligase ligand pomalidomide through a PEG linker [40]. After the development of this degrader, several PROTACs targeting HDAC6 enzyme were developed [41-43].

Recently, the development of class I HDAC targeting PROTACs became interesting. In 2020, Smalley et al. [44] were able to develop a PROTAC able to effect a near complete degradation of HDAC1, 2 and 3. With their work they proved the ability to use PROTACs to target these class I HDACs members which are localized in the nucleus and are a part of large multi-protein complexes. In the same year, Roatsch et al. reported the development of PROTACs based on macrocyclic tetrapeptides degrading HDAC1-3. [45] Another group recently published a first-in-class HDAC3 specific PROTAC [46].

Up to now, PROTACs designed to target class I HDACs were aimed to degrade HDAC1, 2 and 3. Lately, Xiong et al. conducted a study to map the degradability of nine HDACs (HDAC1-8 and 10). They synthesized 48 HDAC-targeting degraders based on four pan-HDAC inhibitors linked to three different ubiquitin E3 ligases through linkers with different chemistry. From the pool of the synthesized degraders, only nine compounds showed degradation activity against HDAC8, but were found to be not selective for HDAC8 (also degrading HDAC6). Quantitative proteomics was applied to evaluate the HDACs' degradability and to map the selectivity profile. One of their important findings was that HDAC6 was the most frequently degraded HDAC followed by HDAC8 then HDAC3. Also, their results showed that ligase and linker



chemistry profoundly affected the degrader selectivity. Recruitment of different ligases through different ligase binders, while retaining the linker and the HDAC binding ligand, resulted in preferences in the degraded HDAC isoform. When retaining both ends of the bifunctional molecule, while changing linker lengths, alterations in the selectivity profiles were noticed. These effects included loss of HDAC degradation activity in some cases [47].

To date, there is no study conducted to design degraders specifically targeting HDAC8 or elucidating the cellular effect of HDAC8 degradation utilizing PROTACs which makes this target very interesting to study. In the present work we aimed at the development of bifunctional molecules that potently and selectively degrade HDAC8, while not affecting the activity of the other HDAC isozymes. A further focus was the analysis of the cellular effects of the PROTACs in neuroblastoma cell lines.

## II. Results and Discussion

### *Design concept*

The developed degraders (**1a-p, Table 1**) were built based on previously published HDAC8 inhibitors possessing IC<sub>50</sub> values in the nanomolar range [48,30] (**Table 3**). In previous studies, we found that benzhydroxamates showed good human HDAC8 inhibitory activity and selectivity over hHDAC1 and 6. Crystallographic studies on the orthologous protein in *Schistosoma mansoni* (smHDAC8) as well as molecular docking studies on human HDAC8 [49] revealed that the selectivity of this series of compounds can be attributed to the fact that the aromatic capping group occupies an HDAC8-specific pocket, which is absent in the other HDAC isoforms. Based on these findings, and the fact that the aromatic capping group of the HDAC inhibitors is facing towards the exit of the binding tunnel it can be used as an attachment point for a

linker. The *p*-position of the phenyl capping group was chosen as an appropriate point for the attachment of the linker (**Figure 2**).

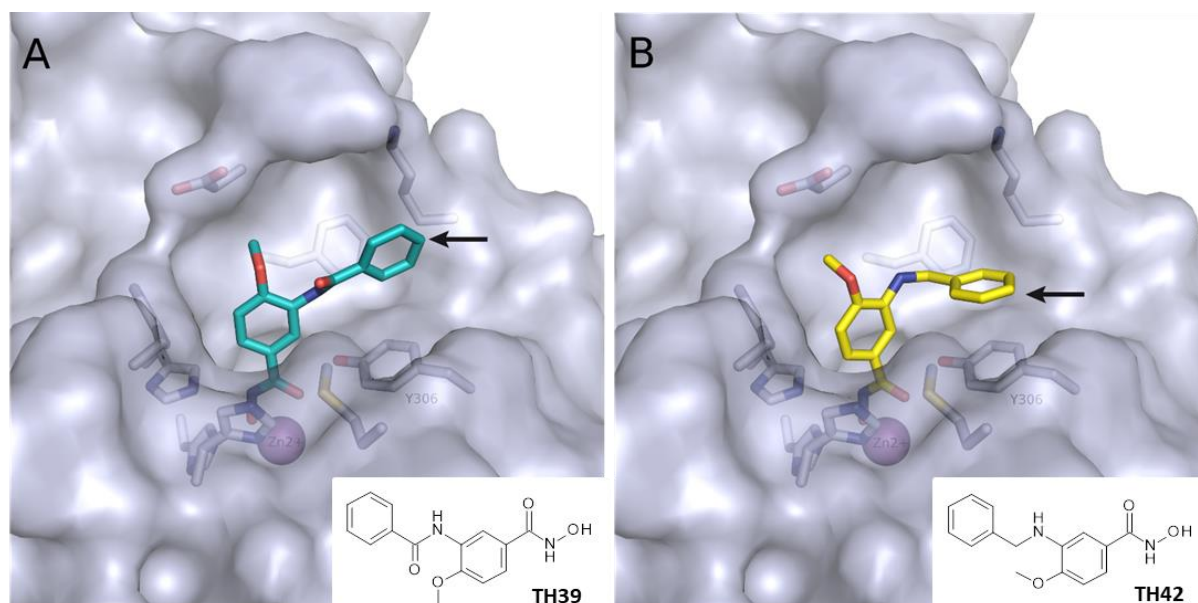


**Figure 2:** Predicted binding mode of A) **2b** (TH39, colored cyan) and B) **2f** (TH42, colored yellow) in human HDAC8 (PDB ID: 6ODB). The arrow indicates the point of linker attachment (*p*-position of the terminal phenyl ring).

The synthesized HDAC8 degraders were designed to act through PROTAC technology or HyT. In several studies, it was proven that the selectivity profile of bifunctional molecules towards protein isoforms that are closely related can be influenced by many factors including the E3 ligase recruited [50,51], the length of the linker [51-54], as well as the point of linker attachment on each of the recruiting units [51,55,56]. The reason is that the formation of the ternary complex is highly affected by these factors. In a trial to increase the probability of the engagement of a ligase by the developed degraders, we used two different ligands to recruit the two E3 ligases which are most utilized in degrader development: the cereblon (CRBN) ligand pomalidomide and a VHL ligand. We also used a variety of linkers, including PEG- and hydrocarbon-based linkers with varying lengths in addition to triazole ring containing linkers. The *in vitro* activity of the synthesized compounds against the

human HDAC enzymes as well as on neuroblastoma cells maintained in culture were determined.

## **Chemistry**

The synthesis of the HDAC degraders (**1a-p, Table 1**) is summarized in **Schemes 1-6**. According to the nature of the linker, the para position of the phenyl cap group of the protected form of the hydroxamic acid based HDAC inhibitor was functionalized. The functionalization at this position should maintain the HDAC binding, as this part of the inhibitor is surface exposed when bound to HDAC8 enzyme.

To synthesize the degraders (**1a-c, 1k and 1m-o, Schemes 1-3**), the protected form of the hydroxamic acid based HDAC inhibitors were synthesized to contain an amino group or an aminomethyl group on the cap phenyl ring. These free amino groups were reacted with the respective carboxylic acid at the terminal part of the aliphatic linker of the E3 ligase ligand-linker-conjugates or adamantane-linker-conjugates (see **Scheme S4.1** in Supp. Info.) forming an amide bond. An exception is **1k (Scheme 2)** where the protected HDAC inhibitor was first linked to the linker through amidation, then the formed protected HDAC inhibitor-linker conjugate was reacted with the VHL ligand to form the protected PROTAC. Finally, the protecting group whether benzyl or 2-tetrahydropyranyl was removed to yield the free hydroxamic acid containing degraders.

For the synthesis of degrader molecules (**1d-f, Scheme 4**) an alkyne functional group was introduced to the protected form of the hydroxamic acid-based inhibitor. On the other hand, conjugates composed of pomalidomide attached through an amide bond to an aliphatic linker terminated with an azide group were synthesized (see **Scheme S4.2** in Supp. Info.). The two units were then attached via azide-alkyne Huisgen

cycloaddition followed by deprotection of the tetrahydropyran protected hydroxamic acid to yield the bifunctional molecules.

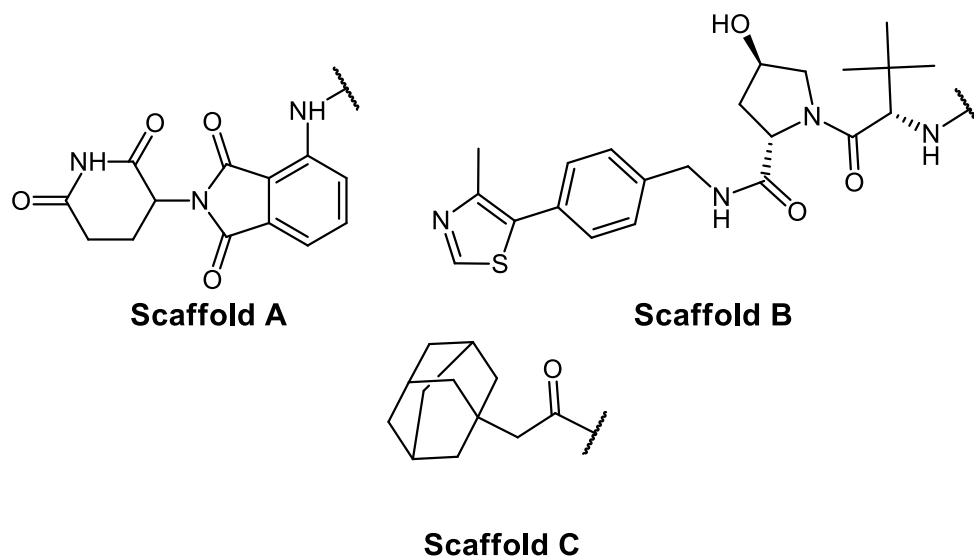
In the degraders (**1g-j**, **1l** and **1p**) whose synthesis is demonstrated in **Schemes 5 and 6** the protected form of the hydroxamic acid based HDAC inhibitor was functionalized in the para position of the cap phenyl ring with a carboxylic acid group. This group was then reacted with the amino-group in the E3 ligase ligand/ HyT-linker conjugate to form an amide bond.

**Scheme 6** displays the synthesis of degraders (**1i** and **1j**). In the first trial of the deprotection step of the benzyl protected degrader through catalytic hydrogenation, Pd/C (10%) was used. This resulted in the unwanted removal of the chlor atom. As a result, in the subsequent deprotection trial, Pd/C (5%) was used which led to the retainment of the halogen. The unexpected degrader molecule formed was then included in the testing to investigate if the absence of the halogen atom in the para-position will affect the degradation profile of the degrader.

In some synthesized degraders (eg. **1a** and **1m**), the HDAC8 inhibitor and the linker were retained, while the entity interacting with the protein degrading machinery was changed. In other cases, both pharmacophores were kept unchanged while the length and/or nature of the linker was changed (eg. **1a** and **1b**; **1g** and **1h**). Also, as shown in **Scheme 4 (1d-f)** we synthesized compounds in which only the HDAC8 inhibitor was changed through different substitution. All these designs were aimed at creating a pool of compounds for the investigation of the effect of the different factors on the degradation ability of the synthesized degraders to optimize the design of a successful HDAC8 degrader.

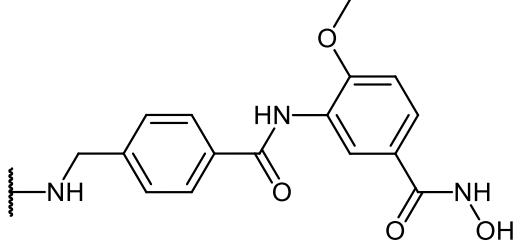
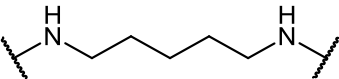
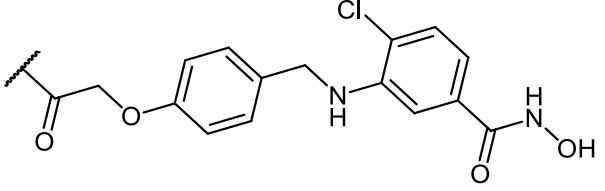
**Table 1** Collection of synthesized degraders.

In total ten CRBN-based PROTACs (**1a-j**), two VHL-based PROTACs (**1k** and **1l**) and four adamantane-based degraders were synthesized (**1m-1p**).

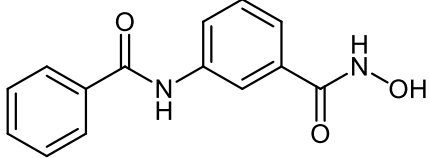
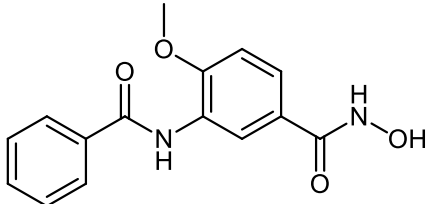
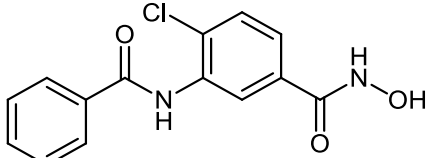
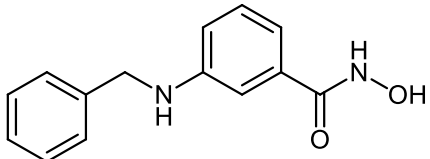
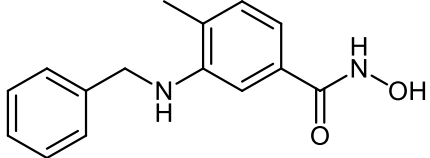
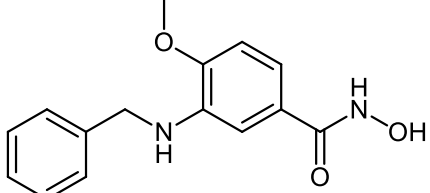


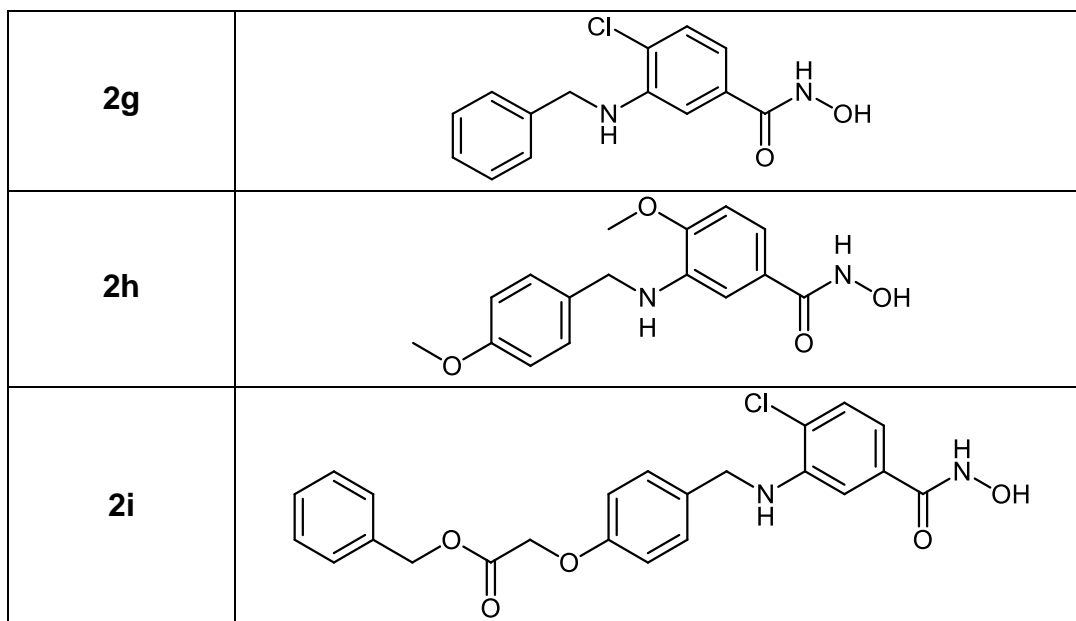
ID	E3 ligase ligand/ HyT ligand	linker	HDAC8 ligand
1a	Scaffold A		
1b			
1c			
1d			

1e			
1f			
1g			
1h			
1i			
1j			
1k	Scaffold B		
1l			
1m	Scaffold C		
1n			

1o			
1p			

**Table 2** Structures of benzhydroxamate-based HADC inhibitors.

ID	Structure
2a	
2b	
2c	
2d	
2e	
2f	



***In vitro* testing:**

**Table 3** IC<sub>50</sub> values for benzhydroxamate-based HDAC inhibitors and synthesized PROTACs.

ID	HDAC1 IC <sub>50</sub> (μM)	HDAC6 IC <sub>50</sub> (μM)	HDAC8 IC <sub>50</sub> (μM)	SI (HDAC1/HDAC8)	SI (HDAC6/HDAC8)
<b>Inhibitors</b>					
<b>2a</b>	33.6 ± 1.8	3.0 ± 0.3	0.58 ± 0.05	58	5
<b>2b</b>	2.3 ± 1.2	2.5 ± 1.1	0.09 ± 0.02	26	28
<b>2c</b>	11.6 ± 3.9	0.12 ± 0.02	0.12 ± 0.04	97	1
<b>2d</b>	2.3 ± 1.2	2.5 ± 1.1	0.14 ± 0.01	16	18
<b>2e</b>	21.8 ± 2.1	5.1 ± 0.3	0.26 ± 0.04	84	20
<b>2f</b>	14.5 ± 1.4	5.1 ± 0.8	0.07 ± 0.02	207	73
<b>2g</b>	10.4 ± 1.2	4.0 ± 0.2	0.25 ± 0.04	42	16
<b>2h</b>	>20	0.15 ± 0.001	0.01 ± 0.001	>2000	15
<b>2i</b>	>20	7.4 ± 0.6	0.41 ± 0.05	>48	18
<b>CRBN-based PROTACs</b>					
<b>1a</b>	4.37 ± 0.65	0.22 ± 0.06	0.09 ± 0.03	49	2



<b>1b</b>	>20	0.56 ± 0.1	0.81 ± 0.17	>24	0.7
<b>1c</b>	10 μM: 40.1 1 μM: 22.2	0.25 ± 0.02	0.15 ± 0.01	-	2
<b>1d</b>	13.1 ± 0.6	6.7 ± 0.6	0.37 ± 0.05	35	18
<b>1e</b>	16.2 ± 0.8	17.2 ± 2.4	0.25 ± 0.07	65	69
<b>1f</b>	10.8 ± 0.7	1.3 ± 0.3	0.25 ± 0.03	43	5
<b>1g</b>	10 μM: 69% 1 μM: 10.1%	10 μM: 72.6% 1 μM: 24.8%	0.59 ± 0.11	-	-
<b>1h</b>	3.91 ± 0.48	10 μM: 66.8% 1 μM: 33.5%	0.33 ± 0.19	12	-
<b>1i</b>	10 μM: 67.4% 1 μM: 20.7%	10 μM: 92.3% 1 μM: 85.4%	0.65 ± 0.14	-	-
<b>1j</b>	10 μM: 60.0% 1 μM: 13.9%	10 μM: 80.9% 1 μM: 46.2%	4.84 ± 1.05	-	-
<b>VHL-based PROTACs</b>					
<b>1k</b>	>20	0.31 ± 0.01	0.11 ± 0.01	>181	3
<b>1l</b>	10 μM: 45.5% 1 μM: 6.0%	10 μM: 72.4% 1 μM: 8.3%	0.72 ± 0.15	-	-
<b>HyT-based PROTACs</b>					
<b>1m</b>	10 μM: 81.9% 1 μM: 47.7%	0.25 ± 0.08	0.57 ± 0.11	-	0.4
<b>1n</b>	10 μM: 30.0% 1 μM: 38.6%	0.82 ± 0.05	0.39 ± 0.03	-	2
<b>1o</b>	10 μM: 52.6 1 μM: 9.8	0.37 ± 0.03	0.09 ± 0.01	-	4
<b>1p</b>	10 μM: 40.0%	10 μM: 72.8%	0.75 ± 0.09	-	-

	1 $\mu$ M: 2.3%	1 $\mu$ M: 12.4%			
--	-----------------	------------------	--	--	--

*In vitro* testing for HDAC-inhibition (see Methods Section for details) showed that the synthesized degraders having 4-substituted 3-aminobenzhydroxamates (e.g. **1d-f**) as HDAC inhibitor part exhibited preference for HDAC8 over the other tested human HDACs (HDAC1 and 6) compared to those degraders possessing 4-substituted 3-amidobenzhydroxamates (e.g. **1b** and **1c**) as warhead which show comparable inhibitory activity against HDAC6 and 8 (**Table 3**).

**1a-f** represent CRBN-based PROTACs. While **1a-c** were designed on the basis of the potent HDAC8 inhibitor **2b**, **1d-f** were synthesized based on the potent HDAC8 inhibitors **2e**, **2f** and **2h** and **2g** respectively. The difference between the degraders **1a-c** is in the length of the linker. While in **1a** there is a six-carbon amide linker attached to the target binding unit, in **1b** the linker is eight carbon long. In the case of **1c**, the unit linking the inhibitor and the E3 ligase part is elongated via the functionalization of the cap group of the inhibitor with aminomethyl group instead of amine group as in **1b**. The HDAC8 inhibitory activity was comparable to the parent inhibitor, in the case of **1a** and **1c**. It decreased in the case of **1b** but remained in the submicromolar range. On the other hand, the selectivity over HDAC6 decreased in the three PROTACs compared to **2b**. In conclusion, the addition of the hydrocarbon-based linker and pomalidomide as an E3 ligase ligand did not affect the inhibition of HDAC8 negatively but led to enhancing the inhibitory activity on HDAC6.

While **1a-c** possess a hydrocarbon chain as a linker, **1d-f** have a triazole containing linker. From the results of the *in vitro* enzymatic assay it can be concluded that the addition of the triazole ring-containing linker and the ligase binding unit did not affect the inhibitory activity on HDAC8. **1d** and **1e** maintained a significant selectivity over

HDAC6, while the selectivity of **1f** over HDAC6 was found to be 3-fold lower than its parent inhibitor **2g**.

The pomalidomide based PROTACs **1g** and **1h** were based on the inhibitor **2e**. Degraders **1g** and **1h**, which only differ in the type of the linker used, showed an almost equipotent activity as the parent inhibitor and significant selectivity over HDAC6. The difference between degrader molecules **1i**, which was designed based on inhibitor **2c**, and **1j** is the absence of the chloro-substituent at position-4 of the benzhydroxamic acid. **1j** is the result of reductive dechlorination which took place during the synthesis of **1i**. The HDAC8 activity was greatly affected and changed from the nanomolar range to the micromolar range further confirming the importance of para-substitution for HDAC8 inhibitory activity. This observation was in accordance with our previous reports [48,30] and further confirm the importance of the para-substitution for HDAC8 inhibitory activity.

**1k** and **1b** differ in the degradation machinery recruiting unit. While **1k** has a VHL-ligand as the E3 ligase binding unit, **1b** bears the CRBN-warhead pomalidomide. Both degraders showed an HDAC8 inhibitory activity with the  $IC_{50}$  values in the submicromolar range. The selectivity over HDAC6 was however lost compared to the parent inhibitor **2b**.

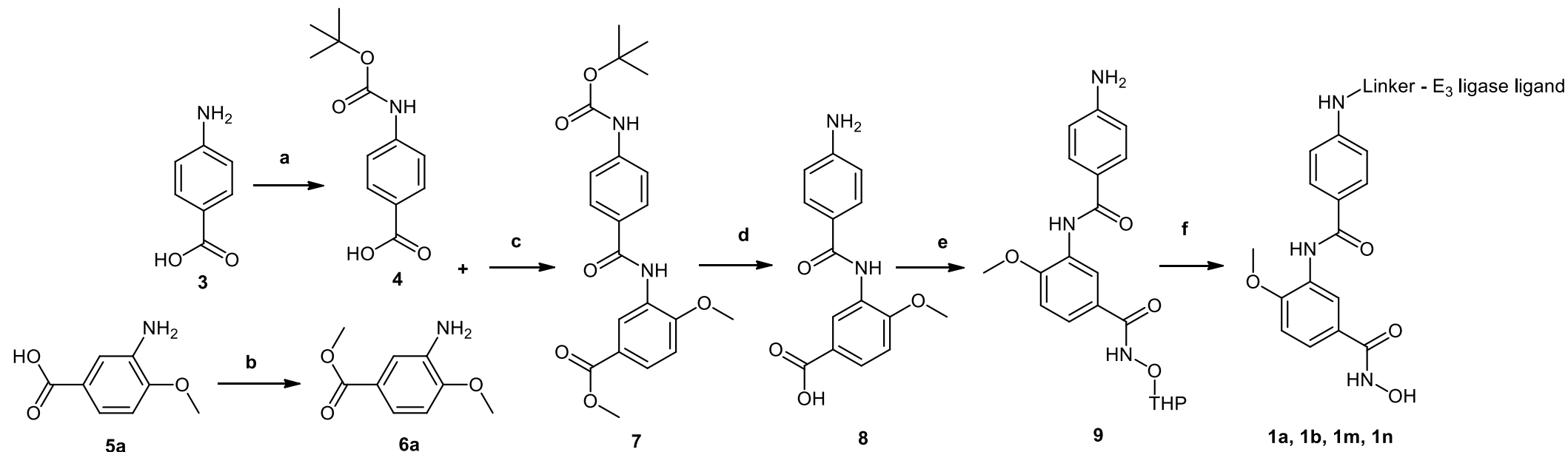
**1m-p** possess adamantane as the degrading machinery engaging unit. In **1m-o** the linker is extended through amide formation with an acetic acid handle bound to the adamantane. In **1o** an elongation of the linker is achieved through the aminomethyl functionalization of the inhibitor's cap group as compared with **1n**. This elongation resulted in an inhibitory activity on HDAC8, comparable to the parent inhibitor **2b** and was accompanied with a 2-fold increase in the selectivity over HDAC6 compared to

**1n**. As their pomalidomide based counterparts **1a-c**, **1m-o** demonstrated good inhibitory activity towards HDAC8 and a significant decrease in the selectivity over HDAC6 compared to the parent inhibitor **2b**.

Interestingly, the addition of the methylene group between the amide group and the cap group of the linker **1c** and **1o** resulted in the improvement of the inhibitory activity against HDAC8 in comparison with **1b** and **1n** respectively, so that the IC<sub>50</sub> values of **1o** and **1c** were similar to that determined for **2b**. Although different ligands for the degrading machinery and different linkers were employed in **1l** and **1p**, both displayed equal inhibitory activity towards HDAC8 and significant selectivity over HDAC6.

Collectively, all synthesized PROTACs, with the exception of the *p*-unsubstituted derivative **1j**, showed HDAC8 inhibitory activity in the submicromolar range which should guarantee the ability of the bifunctional molecules to bind to HDAC8. In addition, the inhibition of HDAC1 was found to be weak. The negative control **33** (see **S2** in Supp. Info.) which possesses a carboxylic ester group instead of the hydroxamic acid group did not demonstrate a strong inhibitory activity against any of the tested HDACs. This confirms the necessity of the presence of a zinc binding group, in this case the hydroxamic acid group, for the degraders/inhibitors to bind to the HDAC enzymes.

**Schemes:**



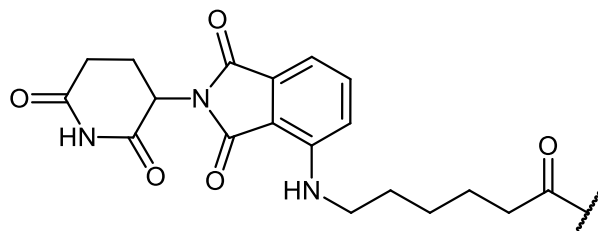
**Compound ID**

**E3 ligase ligand/HyT-linker -**

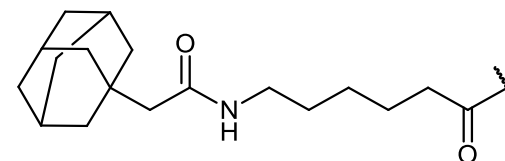
**Compound ID**

**E3 ligase ligand/HyT-linker -**

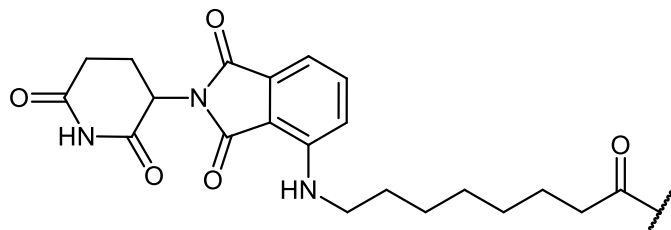
**1a**



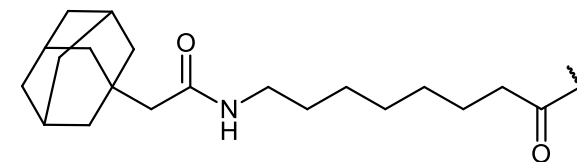
**1m**



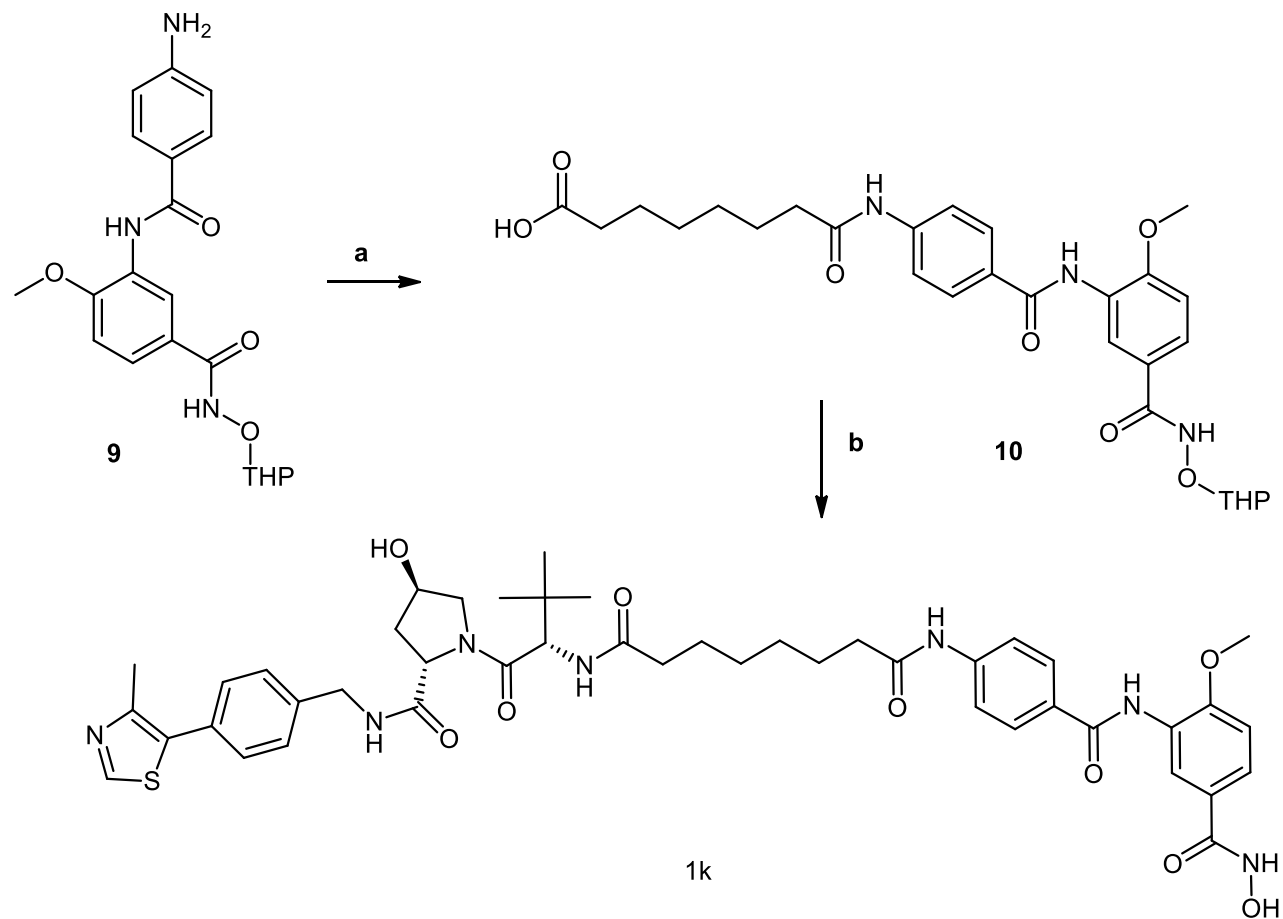
**1b**



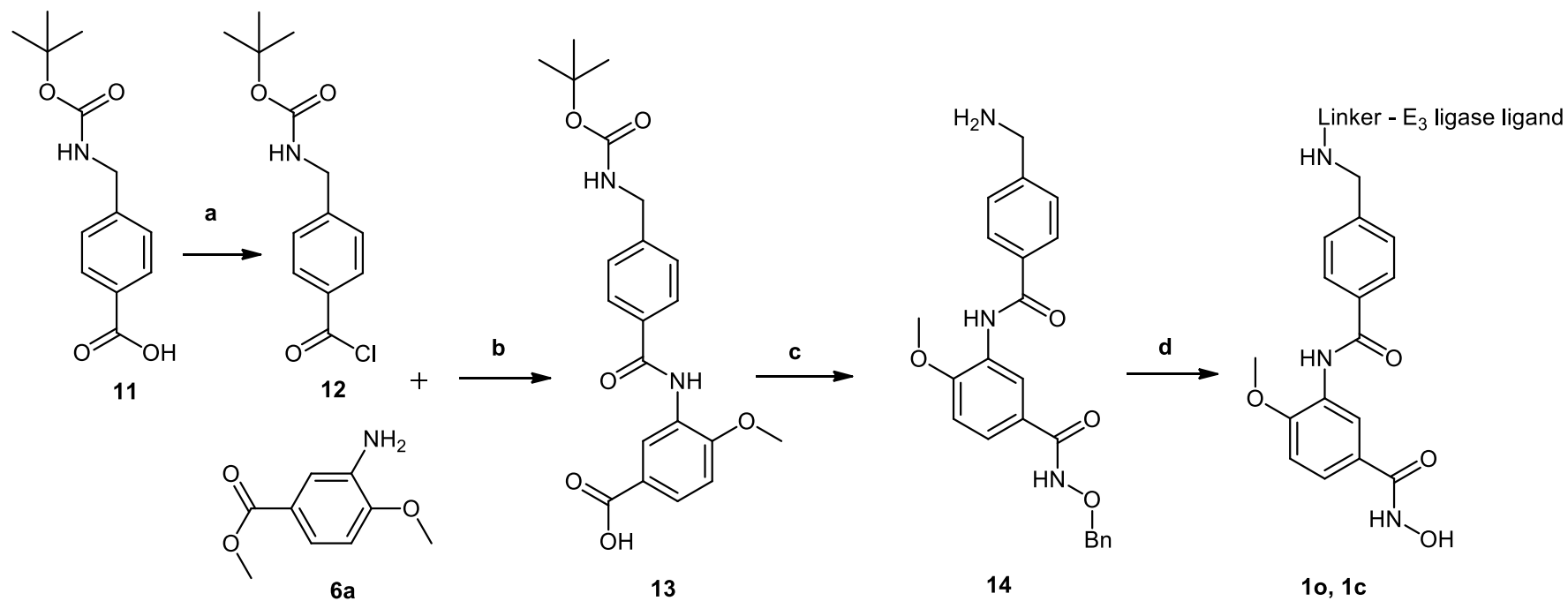
**1n**



**Scheme 1:** Reagents and conditions: (a) TEA, Boc<sub>2</sub>O, 1,4-dioxane, H<sub>2</sub>O, room temperature, 24h; (b) MeOH, SOCl<sub>2</sub>, reflux, 3h; (c) DIPEA, HATU, DMF, 50°C, 24h; (d) 1) 1M NaOH, MeOH, reflux, 2h; 2) TFA, DCM, room temperature, 2h; (e) DIPEA, HATU, NH<sub>2</sub>OTHP, DMF, 50°C, 24h; (f) 1) E3 ligase ligand-linker-COOH **43a,b** / HyT-linker-COOH **47a,b** (see **Scheme S4.1** in Supp. Info.), DIPEA, HATU, DMF, 50°C, 24h; 2) 1M HCl, THF, US, room temperature, 2h.



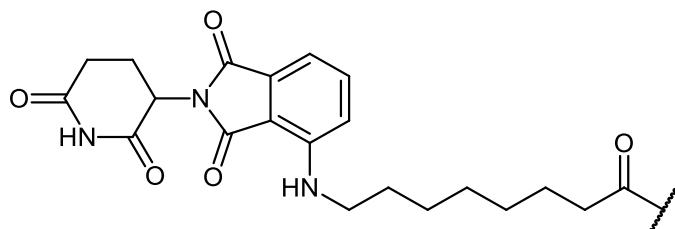
**Scheme 2:** Reagents and conditions: (a) Suberic acid, NMI, TCFH, ACN, room temperature, 24h; b) 1) VHL ligand **40** (see **S3** in Supp. Info.), DIPEA, HATU, DMF, 0°C, 2h; 2) 1M HCl, THF/MeOH, US, 0°C, 2h.



Compound ID

E3 ligase ligand-linker -

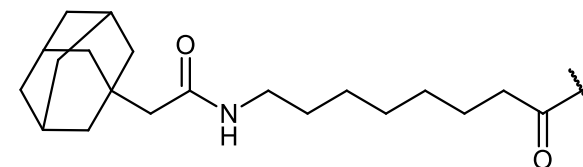
1c



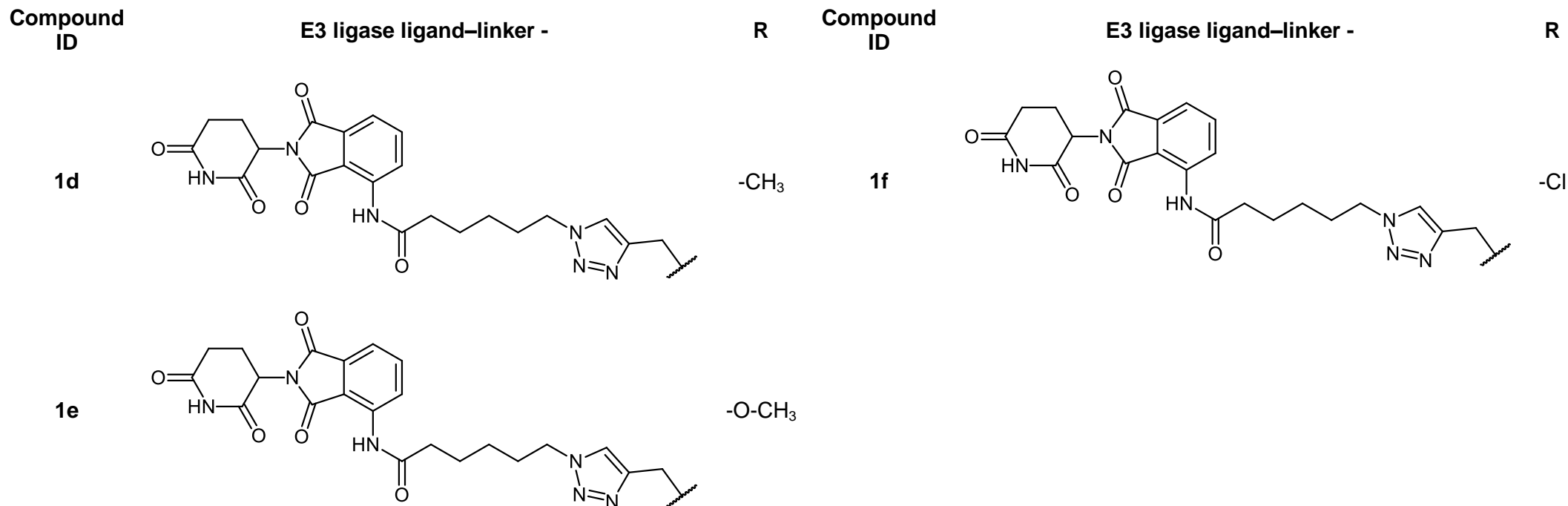
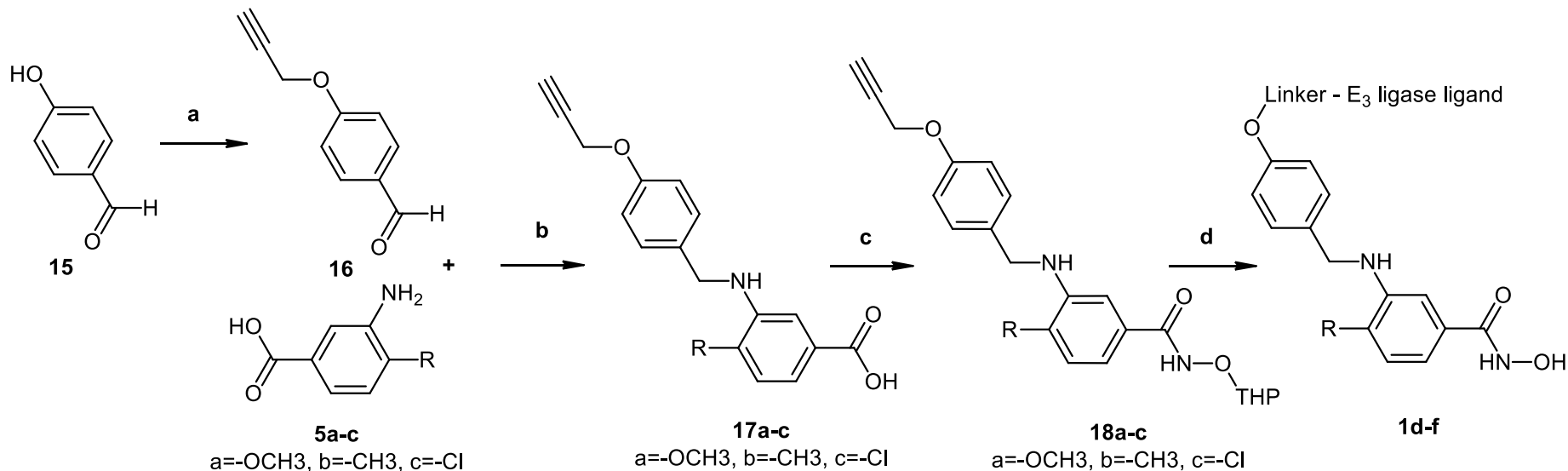
Compound ID

E3 ligase ligand-linker -

1o

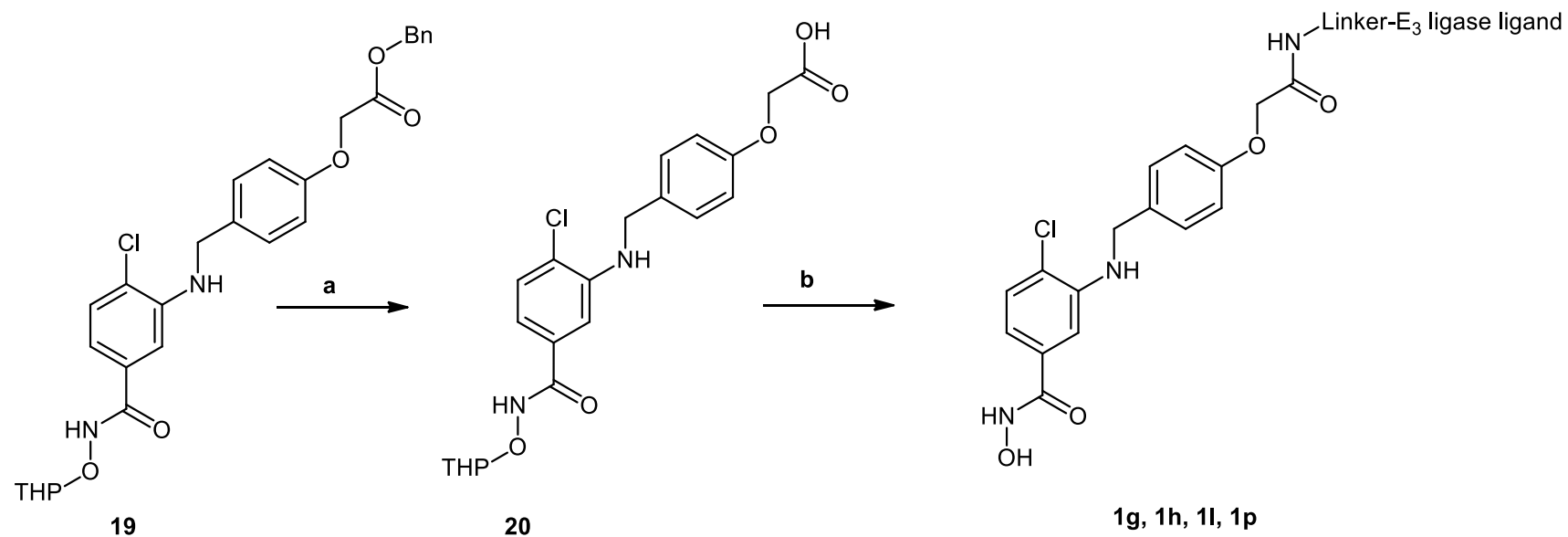


**Scheme 3:** Reagents and conditions: (a) DMF, C<sub>5</sub>H<sub>5</sub>N, C<sub>2</sub>O<sub>2</sub>Cl<sub>2</sub>, room temperature, 6h; (b) 1) C<sub>5</sub>H<sub>5</sub>N, room temperature, 24h; 2) 1M NaOH, MeOH, reflux, 2h; (c) 1) DIPEA, HATU, NH<sub>2</sub>OBn-HCl, DMF, 50°C, 24h; 2) TFA, DCM, room temperature, 2h; (d) 1) E3 ligase ligand-linker-COOH **43b** / HyT-linker-COOH **47b** (see **Scheme S4.1** in Supp. Info.), DIPEA, HATU, DMF, 50°C, 24h; 2) Pd/C (5%), H<sub>2</sub>, THF, 24h.



**Scheme 4:** Reagents and conditions: (a) 1)  $\text{K}_2\text{CO}_3$ , DMF, room temperature, 1hr; 2) propargyl bromide at  $0^\circ\text{C}$ ; 3) 24hrs at room temperature; (b) 1) toluene, reflux, 2hr; 2) THF,  $0^\circ\text{C}$ ,  $\text{CH}_3\text{COOH}$ ,  $\text{Na}(\text{CH}_3\text{COO})_3\text{BH}$ , 30min; 3) 24h, room temperature; (c) DIPEA, HATU,  $\text{NH}_2\text{OTHP}$ , DMF,  $50^\circ\text{C}$ , 24h; (d) 1) E3 ligase ligand-linker-**N**<sub>3</sub> **50** (see **Scheme S4.2** in Supp. Info.), tert-Butanol /  $\text{H}_2\text{O}$ , Sod. Ascorbate,  $\text{CuSO}_4 \times 5\text{H}_2\text{O}$ , 24h, room temperature; 2) 1M HCl, THF, US, room temperature, 2h.

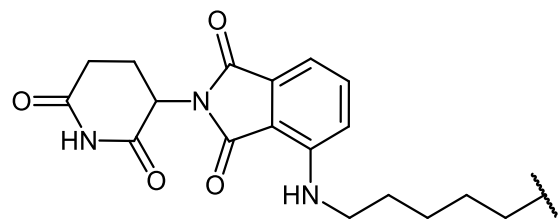




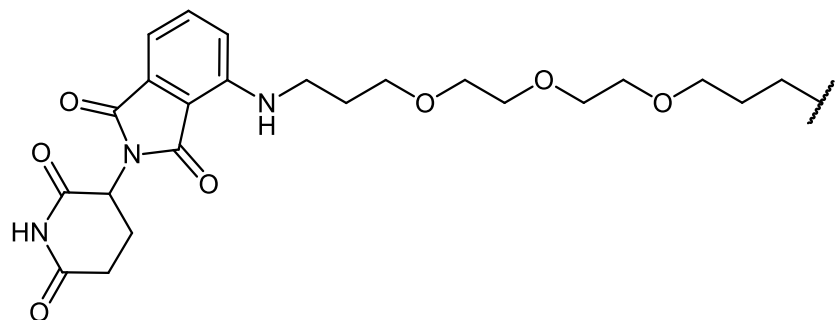
Compound ID

E3 ligase ligand / HyT-linker-

1g



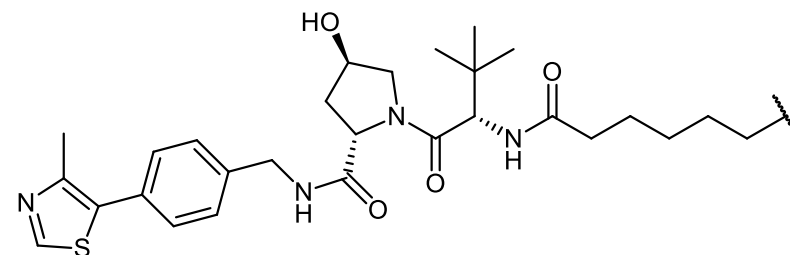
1h



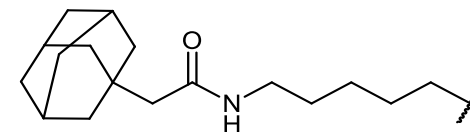
Compound ID

E3 ligase ligand / HyT-linker-

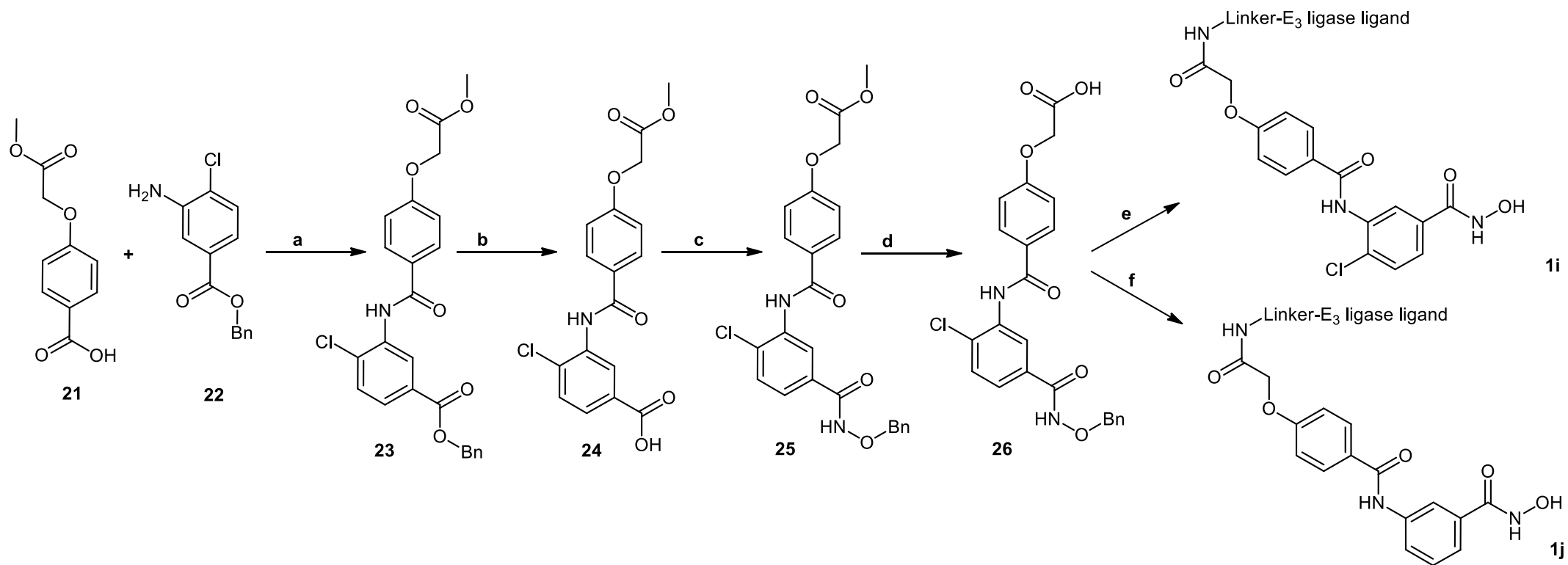
1l



1p



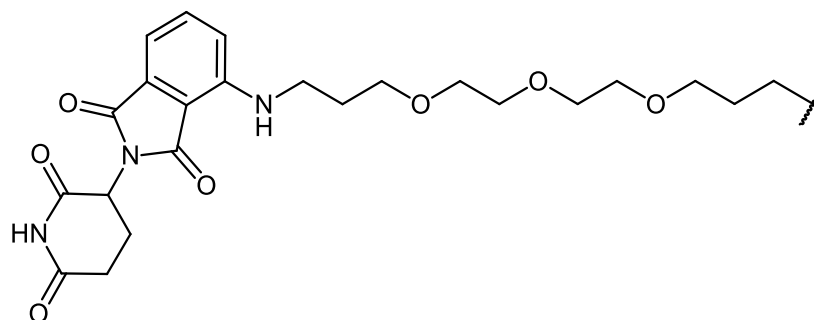
**Scheme 5:** Reagents and conditions: (a) Pd/C (5%), H<sub>2</sub>, EtOAc: THF (1:1); (b) 1) E3 ligase ligand-linker-NH<sub>2</sub> **53**, **56**, **59** / HyT-linker-NH<sub>2</sub> **57** (see **Scheme S4.3** in Supp. Info.), DIPEA, HATU, DMF, room temperature; 2) 2M HCl, THF, room temperature.



Compound ID

E3 ligase ligand-linker -

1i  
1j



**Scheme 6:** Reagents and conditions: (a) 1) SOCl<sub>2</sub>, reflux, 2) DIPEA, THF; (b) Pd/C (5%), H<sub>2</sub>, EtOAc: THF (1:1); (c) DIPEA, HATU, NH<sub>2</sub>OBn·HCl, DMF, room temperature; (d) LiOH, H<sub>2</sub>O: THF (1:1), room temperature; (e) 1) E3 ligase ligand-linker-NH<sub>2</sub> **53** (see **Scheme S4.3** in Supp. Info.), HATU, DIPEA, DMF; 2) H<sub>2</sub>, Pd/C (5%), MeOH. (f) 1) E3 ligase ligand-linker-NH<sub>2</sub> **53** (see **Scheme S4.3** in Supp. Info.), DIPEA, HATU, DMF; 2) H<sub>2</sub>, Pd/C (10%), MeOH.

**Non-enzymatic stability testing for selected final PROTACs**

**Table 4** Non-enzymatic stability data of selected final PROTACs tested in assay medium at 37 °C.

	<b>0h - %</b>	<b>6h - %</b>	<b>12h - %</b>	<b>24h - %</b>	<b>48h - %</b>	<b>72h - %</b>
<b>1a</b>	100	100.7	100.9	99.9	93.4	84.8
<b>1b</b>	100	102.5	103.3	91.6	42.1	11.2
<b>1c</b>	100	99.3	98.3	94.0	87.9	81.2
<b>1e</b>	100	91.6	82.8	65.5	33.8	13.2
<b>1f</b>	100	84.6	67.3	48.3	12.1	2.8
<b>1g</b>	100	99.4	99.8	97.2	89.1	84.2
<b>1h</b>	100	99.5	98.8	95.0	91.0	89.6
<b>1i</b>	100	99.2	98.3	97.4	92.6	88.1
<b>1k</b>	100	102.5	104.2	105.1	105.0	104.3
<b>1l</b>	100	101.4	100.9	101.3	104.1	102.7
<b>1m</b>	100	101.6	102.6	102.6	103.3	103.6
<b>1n</b>	100	101.6	103.2	103.8	104.6	104.6
<b>1o</b>	100	99.9	101.2	95.9	96.7	95.4
<b>1p</b>	100	102.5	103.8	103.9	105.3	105.8

To test the chemical/biochemical stability of the developed PROTACs we set up a non-enzymatic stability assay. Compounds were diluted in one of these assay media; Dulbecco's Modified Eagle Medium (DMEM) (50%)/dimethylsulfoxid (10%)/acetonitrile (40%) or DMEM (50%)/dimethylsulfoxid (10%)/methanol (40%) and incubated at 37 °C for max. 72 h. The results of the non-enzymatic stability testing are presented in **Table 4** and **S8** in the **Supp. Info**. In the applied conditions, most tested compounds were stable over 72 h at the physiological pH 7.4 and 37 °C, with a maximum percentage of decomposition of ~20%. **1b**, and **1e** were stable for 24 h but showed some degradation after 72h. **1f** was the least stable compound and was decomposed at the end of the 72h testing period.

Generally, the nature and length of the linker and its connection points with both ligands greatly affect the stability of the complex molecule of the PROTACs [57-60]. Studies show that thalidomide [61] and its derivative pomalidomide can undergo non-enzymatic rapid hydrolysis at the four amide bonds of the phthalimide and glutarimide rings [57]. However, the stability of thalidomide derivatives as a component of a PROTAC molecule is significantly affected by the different linker junctions [57,58]. This explains that although **1a**, **1c**, and **1g-1i** exhibit pomalidomide as the E3 ligase ligand, they are more stable than **1b**, **1e** and **1f** over the period of the testing.

The difference between the less stable **1b** and the stable **1c** lies in the cap group of the inhibitor. While in **1b** the cap group contains an amine in the para-position, in **1c** an aminomethyl group is present. The addition of the methylene group seems to increase the stability of the amide group joining the linker with the HDAC inhibitor.

### Cellular testing

To test the potential toxicity of the *in vitro* active PROTACs, cytotoxicity tests were performed on human embryonic kidney-derived HEK293 cells. As shown in **Table 5**, the HDAC8 inhibitors and PROTACs showed weak to no cytotoxic effects against HEK293 cells at a high concentration of 50  $\mu$ M.

**Table 5** Cytotoxicity on HEK293 cells (cell viability at 50  $\mu$ M inhibitor treatment).

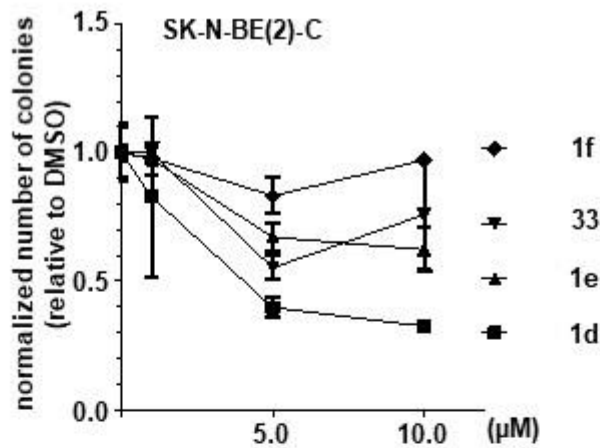
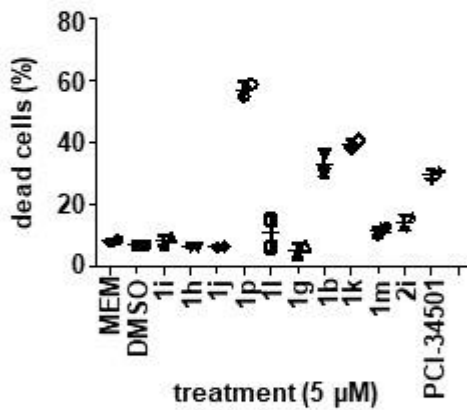
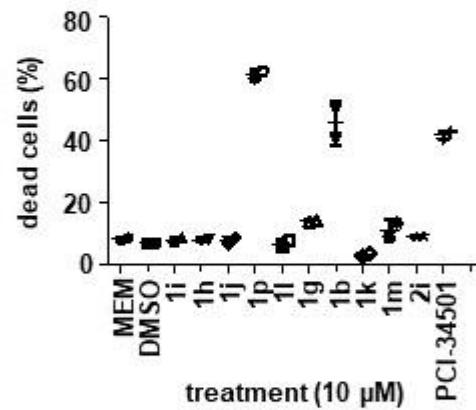
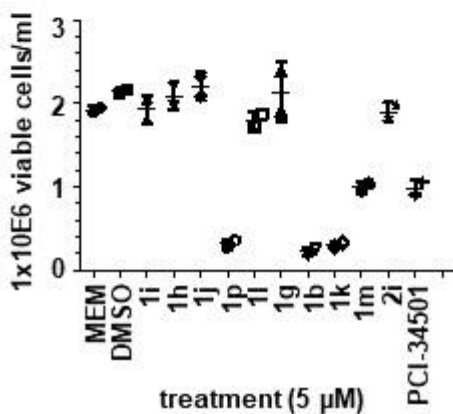
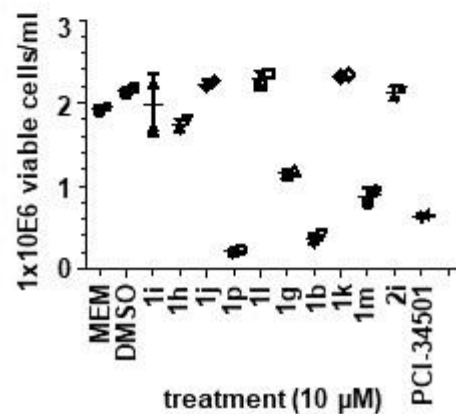
ID	HEK293 viability 50 $\mu$ M	ID	HEK293 viability 50 $\mu$ M	ID	HEK293 viability 50 $\mu$ M
<b>2a</b>	72.0 $\pm$ 2.9	<b>1a</b>	85.6 $\pm$ 2.4	<b>1j</b>	83.7 $\pm$ 3.5
<b>2b</b>	67.3 $\pm$ 3.9	<b>1b</b>	64.1 $\pm$ 1.7	<b>1k</b>	78.2 $\pm$ 3.7
<b>2c</b>	72.2 $\pm$ 3.5	<b>1c</b>	70.1 $\pm$ 6.7	<b>1l</b>	90.4 $\pm$ 2.3
<b>2d</b>	78.8 $\pm$ 6.1	<b>1d</b>	80.2 $\pm$ 2.8	<b>1m</b>	51.5 $\pm$ 6.2
<b>2e</b>	90.4 $\pm$ 1.7	<b>1e</b>	65.1 $\pm$ 4.3	1n	60.0 $\pm$ 3.7
<b>2f</b>	68.1 $\pm$ 1.2	<b>1f</b>	100.5 $\pm$ 2.8	<b>1o</b>	69.3 $\pm$ 1.2
<b>2g</b>	87.4 $\pm$ 3.4	<b>1g</b>	68.2 $\pm$ 2.5	<b>1p</b>	80.1 $\pm$ 1.9
<b>2h</b>	70.4 $\pm$ 7.5	<b>1h</b>	61.3 $\pm$ 0.9		
<b>2i</b>	88.1 $\pm$ 0.1	<b>1i</b>	97.6 $\pm$ 7.0		

### Testing on neuroblastoma cells

To test the effect on neuroblastoma cells, a colony formation assay using SK-N-BE(2)-C cells was performed. Cells were treated with 5 and 10  $\mu$ M of each of the selected PROTACs for 96 h, followed by culturing for another 6 days without treatment (**Figure 3A**). This assesses whether the treatment impairs the clonogenic growth

capacity of tumor cells, indicating effectiveness of compounds on the survival and proliferation of tumor cells. **1d** and **1e** showed the strongest effect on the colony formation.

Moreover, we treated IMR32 p53wt cells with the other PROTACs for 72 hours and counted the remaining viable cells. We quantified the percentage of dead cells as these cells, in contrast to SK-N-BE(2)-C (TP53mut) undergo cell death upon HDAC8 inhibition (**Figure 3B-C**). **1b** and **1p** significantly decreased the ability to form colonies at 5 and 10  $\mu$ M concentrations. In case of **1k** and **1m** the results were less significant whereas the remaining PROTACs were inactive. A similar trend was observed for the cell proliferation assessed via counting of viable cells (**Figure 3D-E**). As reference, the HDAC8 inhibitor PCI-34501 was used [30].

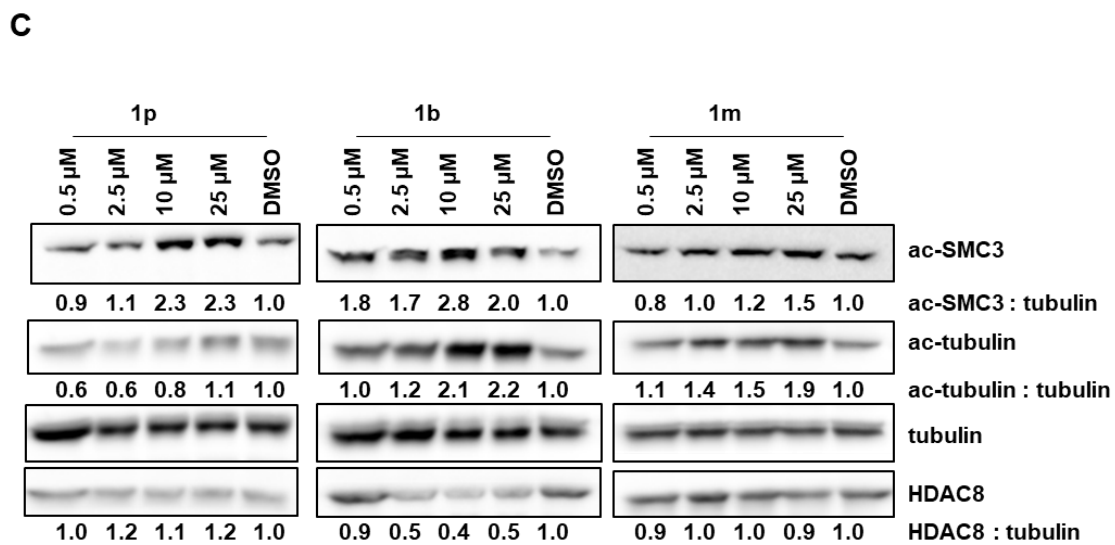
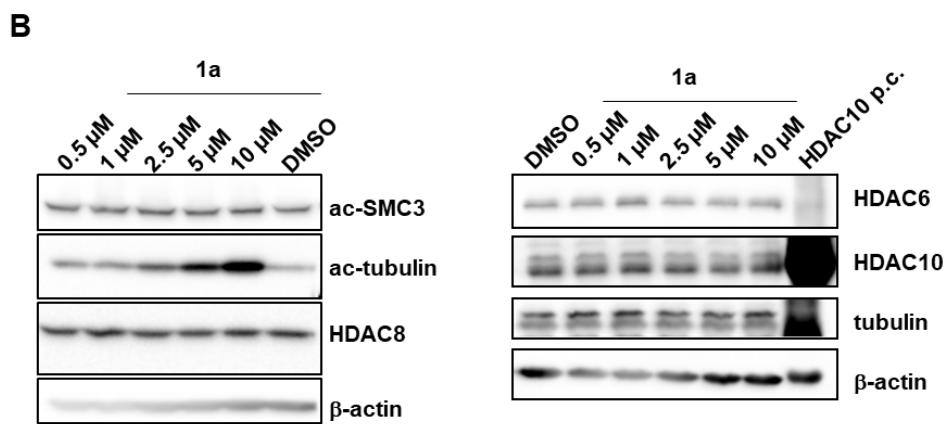
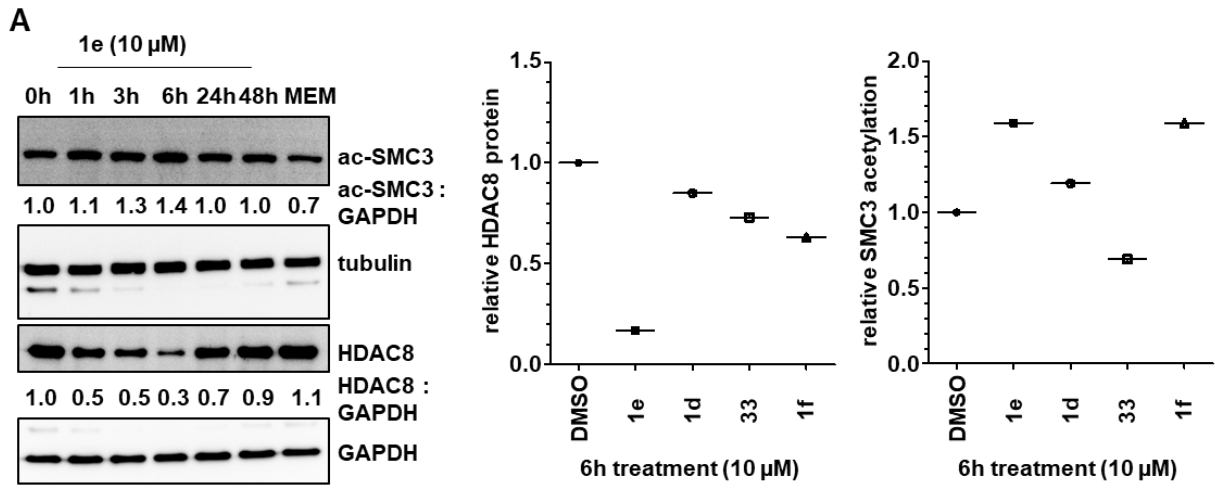
**A****B****C****D****E**

**Figure 3:** **A)** SK-N-BE(2)-C cells; Colony Assay, 10 days (compound treatment within first 96h). Stained with crystal violet and quantified with ImageJ. **B-C)** Trypan Blue assay for detection of dead cells. Neuroblastoma IMR-32 cells were either treated with 5 μM (**B**) or 10 μM (**C**). **D-E)** Cell proliferation assessed via counting of viable cells. IMR-32 cells were either treated with 5 μM (**D**) or 10 μM (**E**) PROTACs.

HDAC8i PCI-34501 served as a positive control, untreated (MEM) and solvent (DMSO) treated cells as negative controls.

To test the degradation of HDAC8 with the developed PROTACs, we selected the most promising compounds obtained from the *in vitro* or neuroblastoma testing, namely **1a**, **1b**, **1d**, **1e**, **1f**, **1m** and **1p**. Whole cell lysates from treated SK-N-BE(2)-C neuroblastoma cells were taken and the protein levels for HDAC8 and the acetylation of its substrate SMC3 were determined (**Figure 4**). As a control for HDAC6, we also assessed acetylation levels of  $\alpha$ -tubulin. It revealed that 6h treatment and a concentration of 10  $\mu$ M gives the highest degradation of HDAC8 and SMC3 acetylation for **1b**, **1e** and **1f** in SK-N-BE(2)-C cells (**Figure 4A, 4C**). As expected, the negative control **33** (bearing a carboxyl ester instead of the hydroxamic acid) did not show hyperacetylation of SMC3 or HDAC8 degradation. Also, **1a**, **1d**, **1m** and **1p** failed to degrade HDAC8 in this neuroblastoma cell line (**Figure 4A-C**). Selected PROTACs were also tested whether they are able to degrade HDAC6 (**Figure 4B, 4D**) but all were shown to be inactive. As positive control we used a recently developed HDAC6 PROTAC [62] (**Figure 4D**).





D

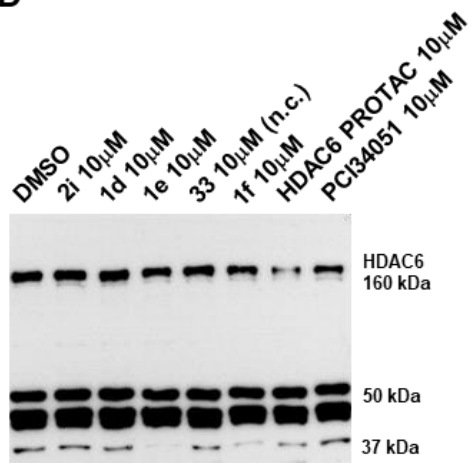


**Figure 4:** A) SK-N-BE(2)-C neuroblastoma cells were treated for indicated time points with 10 μM **1e**. Degradation of HDAC8 and acetylation of HDAC8 target was analysed via western blot. B) SK-N-BE(2)-C neuroblastoma cells were treated for 6h with **1a** at the concentrations given in the figure. Degradation of HDAC8 and acetylation of HDAC8 target SMC3 as well as degradation of HDAC6 and HDAC10 and acetylation of HDAC6 target tubulin was analysed via western blot. A lysate of HDAC10 overexpressing IMR-32 neuroblastoma cells was used to identify the HDAC10 band. C) SK-N-BE(2)-C neuroblastoma cells were treated for 6h with **1b**, **1p** and **1m** at the concentrations given in the figure. Degradation of HDAC8 and acetylation of HDAC8 target SMC3 as well as acetylation of HDAC6 target tubulin was analysed via western blot. D) SK-N-BE(2)-C neuroblastoma cells were treated for 6h with PROTACs **1d**, **1e**, **1f**, the negative control (n.c.) **33**, a HDAC6 PROTAC [62] and the two inhibitors **2i** and **PCI34051** at the concentrations given in the figure. Degradation of HDAC6 was analysed via western blot.

As HDAC8 inhibition is known to induce signs of neuronal differentiation, such as neurite-like outgrowths in neuroblastoma cells [21]), we treated SK-N-BE(2)-C cells with **1b**, **1e**, **1k**, **1m** and **1p** for 6-10 days then stained the cells with crystal violet to visualize neurite-like outgrowths. For comparison, we treated the cells with the known neuronal differentiation inducer retinoic acid (ATRA) which is a known drug, that is applied for neuroblastoma treatment under some circumstances. We also combined

one PROTAC, namely **1e** with ATRA, which substantially enhanced the differentiation phenotype (**Figure 5**). These results are in line with the published differentiation enhancement (longer outgrowths, more cells with outgrowths in combination) effect of PCI-34051 [21].

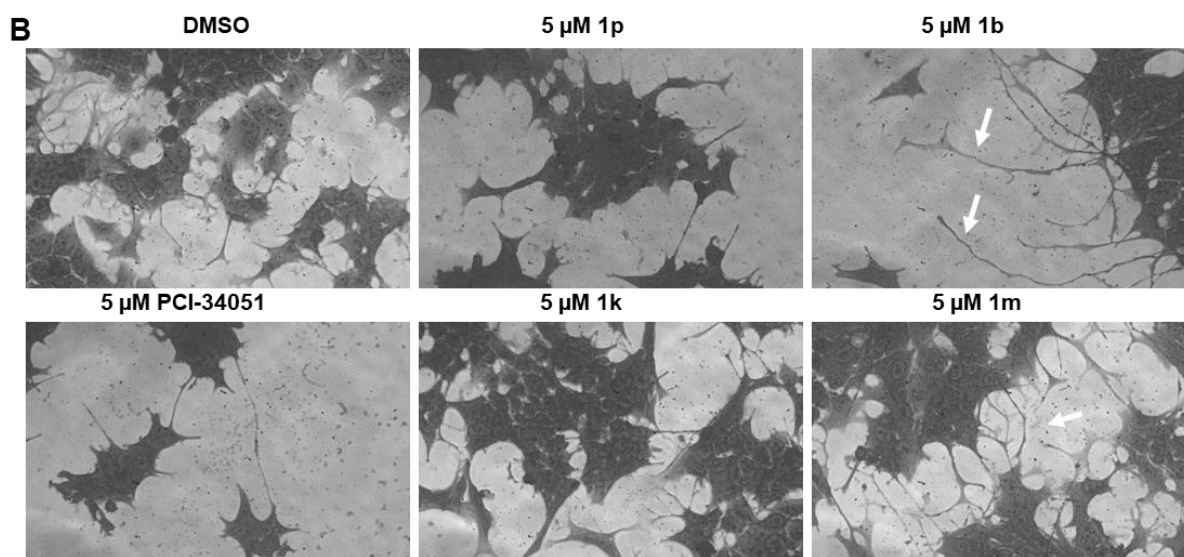
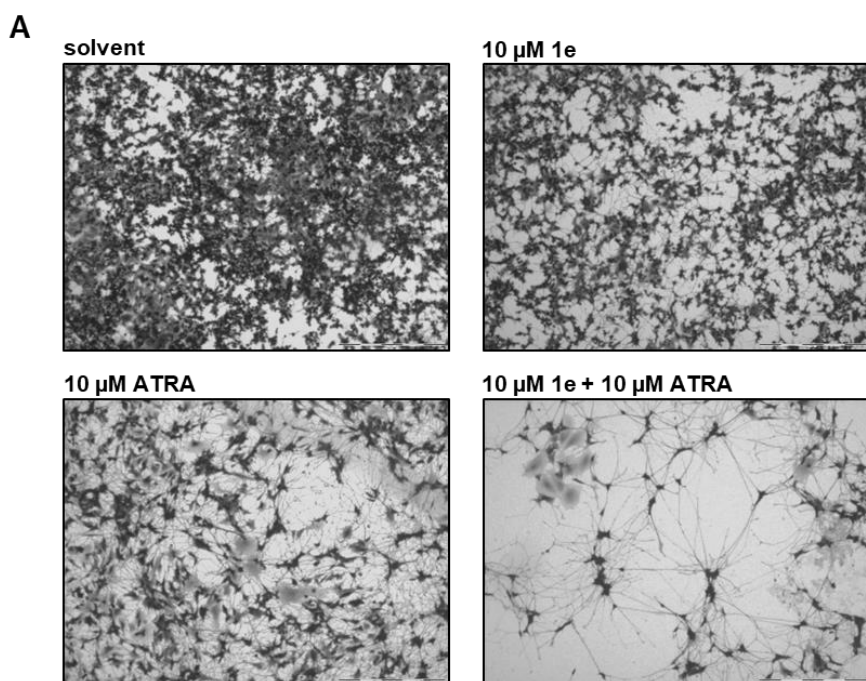


**Figure 5:** A) SK-N-BE(2)-C cells, treated for 10 days. Scale bar: 500  $\mu\text{m}$ . Stained with crystal violet. B) SK-N-BE(2)-C cells, treated for 6 days. Stained with crystal violet.

## Conclusion

In summary, we designed a pool of bifunctional degraders based on previously published HDAC8 inhibitors with good inhibitory activity. Different linker types and lengths in addition to various degradation machinery recruiting units were employed to evaluate the effect of the various factors on the binary engagement of the degrader molecule with the targeted HDAC8 enzyme. The effect of these factors on the degradation ability of the synthesized degraders was also determined through testing them on SK-N-BE(2)-C cells neuroblastoma cells and determination of the protein levels for HDAC8 and the acetylation of its substrate SMC3. From the synthesized compounds the CRBN based PROTACs **1b** and **1e** resulted in strong HDAC8 degradation connected with SMC3 acetylation after 6h treatment when used at a concentration of 10  $\mu\text{M}$ . HDAC6 was not degraded by the developed PROTACs. Besides the good degradation effects of the small molecule-based degraders **1b** and **1e**, these two compounds also exhibited good anti-neuroblastoma activity. With our study we aim to provide a basis for future chemical optimization of degrader molecules targeting specifically the HDAC8 enzyme.

## **I. Materials and methods**

### **1. General**

All materials and reagents were purchased from Sigma-Aldrich Co. Ltd. and abcr GmbH. All solvents were analytically pure and were dried before use. Thin layer chromatography was carried out on aluminium sheets coated with silica gel 60 F254 (Merck, Darmstadt, Germany). For medium pressure chromatography (MPLC) silica gel Biotage<sup>®</sup> SNAP ultra-HP-sphere 25 µm containing columns were used.

Chloroform:methanol; n-hexane:ethyl acetate or ethyl acetate:acetonitrile were the elution systems used for medium pressure chromatography. Triethylamine was added in a concentration of 0.1 % to chloroform or ethyl acetate, according to the solvent system used, in purification of compounds protected with 2-tetrahydropyranyl group.

In the preparative high-pressure chromatography used for cleaning of the final PROTACs, LiChrosorb<sup>®</sup> RP-18 (7 µm) 250-25 Merck column was used. The applied mobile phase was a gradient with increasing polarity composed of acetonitrile/water.

Final compounds' purity was determined using high-pressure chromatography (HPLC). Purity was measured by UV absorbance at 254 nm. Two analytical methods were used while determining the purity. In the first method (M1), the components of the HPLC were an XTerra RP18 column (3.5 mm, 3.9 mm x 100 mm) from the manufacturer Waters (Milford, MA, USA) and two LC-10AD pumps, a SPD-M10A VP PDA detector, and a SIL-HT autosampler, all from the manufacturer Shimadzu (Kyoto, Japan). In the second method (M2), only the column was changed to LiChrosorb<sup>®</sup> RP-18 (5 µm) 100-4.6 Merck column.

Mass spectrometry analyses were performed with a Finnigan MAT710C (Thermo Separation Products, San Jose, CA, USA) for the ESIMS spectra and with an LTQ (linear ion trap) Orbitrap XL hybrid mass spectrometer (Thermo Fisher Scientific, Bremen, Germany) for the HRMS-ESI (high resolution mass spectrometry) spectra. For the HRMS analyses, the signal for the isotopes with the highest prevalence was given and calculated ( $^{35}\text{Cl}$ ,  $^{79}\text{Br}$ ).

$^1\text{H}$  NMR and  $^{13}\text{C}$  NMR spectra were taken on a Varian Inova 500 using deuterated chloroform or deuterated dimethylsulfoxide as solvent. Chemical shifts are referenced to the residual solvent signals.

Non-enzymatic stability of selected final compounds was determined using 10  $\mu\text{M}$  concentration of the tested PROTACs in one of the following assay media; Dulbecco's Modified Eagle Medium (DMEM) (50%)/ Dimethylsulfoxid (10%)/ acetonitrile (40%) or DMEM (50%)/ Dimethylsulfoxid (10%)/ methanol (40%) mixture at pH7.4. In case of TH166 Methanol was used instead of acetonitrile due to solvent problems. The formed solution mixtures were incubated for 0, 6, 12, 24, 48 and 72h at 37°C. Analyte decomposition was monitored by HPLC using XTerra RP18 column (3.5 mm, 3.9 mm x 100 mm) from the manufacturer Waters (Milford, MA, USA) and two LC-10AD pumps, a SPD-M10A VP PDA detector, and a SIL-HT autosampler, all from the manufacturer Shimadzu (Kyoto, Japan).

## **2. General synthetic methods**

### **Method I, reductive amination**

- A.** A mixture of the benzaldehyde (1 eq.) and the amine (5% molar excess) was dissolved in toluene and was heated under reflux using a water trap for 2h. Afterwards the solvent was removed under reduced pressure. The remaining

residue was dissolved in dry tetrahydrofuran and the formed solution was cooled to 0°C. Glacial acetic acid (2 eq.) was added followed by sodium triacetoxyborohydride (4 eq.) and the reaction mixture was stirred for 30 minutes at 0°C. Afterwards the ice bath was removed and stirring was continued for 24h at room temperature. The reaction was then quenched by the addition of sodium bicarbonate and the product was extracted with ethyl acetate. The organic layer was washed with 1M hydrochloric acid followed by brine and was dried over anhydrous sodium sulfate. Finally, it was filtered and evaporated under reduced pressure. The crude product was purified using the MPLC. The yields were in the range 60%-95%.

- B.** A mixture of benzaldehyde (1.1 eq.), the corresponding amine (1 eq.), trifluoroacetic acid (2 eq.), and sodium triacetoxyborohydride (1.2 eq.) was dissolved in a mixture of tetrahydrofuran and ethyl acetate (1:1). After stirring the reaction mixture at room temperature for 2h, the reaction was quenched by adding water and the crude product was extracted with ethyl acetate. The combined organic layer was dried over anhydrous sodium sulfate, filtered, and concentrated in vacuo. The crude residue was purified using MPLC. The yield was around 50%.

## **Method II, ester hydrolysis**

- A.** To a solution of the methyl ester (1 eq.) in methanol, 1M aqueous sodium hydroxide (10 eq.) was added. The formed reaction mixture was refluxed for 2-4h. After complete ester hydrolysis, the solvent was evaporated under reduced pressure to yield a crude residue that was dissolved in water. The aqueous solution was extracted using ethyl acetate to remove any organic impurities. In the next step, 1M aqueous hydrochloric acid (10 eq.) was added to the aqueous

solution to liberate the free acid which was extracted using ethyl acetate. The combined organic layer was washed with brine and dried over anhydrous sodium sulfate. It was then filtered, and the solvent was evaporated under reduced pressure to give the crude product which was purified using the MPLC. The yields were 70%-96%.

- B.** To the suspension of the methyl ester (1 eq.) in a mixture of tetrahydrofuran and water (1:1) lithium hydroxide (5 eq.) was added. The mixture was stirred at room temperature until complete hydrolysis of the ester then tetrahydrofuran was evaporated. Using aqueous 1M hydrochloric acid, the pH of the remaining aqueous solution was adjusted to pH 6. The liberated free acid was extracted using a mixture of ethyl acetate and tetrahydrofuran. The combined organic layer was then dried over anhydrous sodium sulfate, filtered, and concentrated in vacuo to yield the product, which required no further purification. Crude yields were around 80-90%.

### **Method III, amide bond formation**

- A.** A solution of the carboxylic acid (1-1.2 eq.) and *N,N*-diisopropylethylamine (3 eq.) in dimethylformamide was stirred for 15 min at room temperature then 1-[bis(dimethylamino)methylene]-1H-1,2,3-triazolo[4,5-b] pyridinium 3-oxid hexafluorophosphate (1.2-1.5 eq.) was added and stirring was continued for another 30 min. Next, the corresponding amine (1-1.5 eq.) was added to the solution. The formed reaction mixture was stirred at 0°C or at room temperature or at 50°C for 2-24h. After completion of the reaction, water was added to the reaction mixture and the formed solution was extracted using ethyl acetate. The combined organic layer was washed with aqueous 1M sodium bicarbonate solution followed by aqueous 1M ammonium chloride solution and brine. After



drying over anhydrous sodium sulfate, the organic layer was filtered then concentrated in vacuo to yield the crude compound which was purified using MPLC. The yields were around 27-100%.

- B.** To a suspension of the carboxylic acid (1 eq.) in toluene, drops of dimethylformamide were added followed by pyridine then oxalyl chloride (2 eq.). The reaction mixture was stirred at room temperature for 6h. The formed precipitate was then filtered and washed with toluene. Afterwards, the combined organic filtrates were concentrated under reduced pressure to give the acid chloride that was used directly without further purification. It was dissolved in pyridine and the amine (1 eq.) was added to the solution. The formed reaction mixture was stirred at room temperature for 24h. After evaporation of the solvent the remaining residue was dissolved in chloroform and was successively washed with 10% hydrochloric acid, 1M sodium bicarbonate and brine. After drying the organic layer over anhydrous sodium sulfate, it was evaporated under reduced pressure to give the crude product which was purified using the MPLC. The yield was around 48%.
- C.** After the dropwise addition of thionyl chloride (3 eq.) to the carboxylic acid (1 eq.) at 0 °C, the reaction mixture was heated under reflux for 2h then the excess thionyl chloride was evaporated under vacuum. The formed acid chloride was dissolved in dry tetrahydrofuran and was added dropwise to a solution of the corresponding amine (0.9 eq.) and *N,N*-diisopropylethylamine (3 eq.) in tetrahydrofuran. The reaction mixture was stirred at room temperature till completion. Afterwards it was diluted with ethyl acetate and was washed with a saturated aqueous solution of ammonium chloride followed by brine. Finally, the organic layer was dried over anhydrous sodium sulfate, filtered, and concentrated

in vacuo to obtain the crude residue which was purified using MPLC. The yield was around 50-70%.

- D.** A mixture of the carboxylic acid (3 eq.), *N*-methylimidazole (3.5 eq.) and chloro-*N,N,N',N'*-tetramethylformamidinium-hexafluorophosphate (1.2 eq.) were stirred in acetonitrile for 15 min. The amine (1 eq.) was dissolved in some acetonitrile then was added to the mixture. The formed reaction mixture was stirred at room temperature for 20 hr. After completion of the reaction was confirmed by TLC, water was added, and the mixture was extracted using ethyl acetate. The combined organic layer was washed with water followed by brine. After drying over anhydrous sodium sulfate, the organic layer was filtered then concentrated in vacuo to yield the crude compound which was purified using MPLC. The yield was around 67%.

#### **Method IV, azide-alkyne Huisgen cycloaddition**

In a two-necked flask, a mixture of azide containing conjugate (1 eq.), propargyl group containing ligand (1 eq.), sodium ascorbate (0.2 eq.) and copper(II) sulfate pentahydrate (0.2 eq.) was dissolved in a solvent mixture composed of tetrahydrofuran and water (2:1). After purging the reaction mixture with argon, the flask was placed in the dark and the mixture was stirred for 24h at room temperature. After the completion of the reaction, the solvent was evaporated under reduced pressure. The remaining residue was dissolved in 1M aqueous ammonium chloride, and the formed aqueous solution was extracted with ethyl acetate. The combined organic layer was washed with brine then it was dried over anhydrous sodium sulfate. Finally, the solvent was evaporated under reduced pressure to yield the crude product which was purified using the MPLC. The yield was around 67-70 %.

### **Method V, deprotection of tetrahydropyranyl ether**

To a solution of the 2-tetrahydropyranyl-protected product (1 eq.) in tetrahydrofuran or tetrahydrofuran with few drops of methanol, 10-15 drops of 1M hydrochloric acid were added, and the reaction mixture was sonicated at 0°C or room temperature for 2h or until TLC showed completion of the reaction. The solvent was then evaporated under vacuum and the crude product was purified by preparative HPLC. The yields were around 20-50%.

### **Method VI, deprotection of tert-butyl protected carbamates and tert-butyl ester protected carboxylic acids**

To a solution of tert-butyl protected carbamate (1 mmol) or tert-butyl ester protected carboxylic acid (1 mmol) in dichloromethane, trifluoroacetic acid (1 mL) was added. The reaction mixture was then stirred at room temperature for 2-24h. After completion of the reaction, the solvent and excess trifluoroacetic acid were evaporated under reduced pressure to yield the crude product which was purified using the MPLC. The yields were around 78-100%.

### **Method VII, catalytic hydrogenation**

A mixture of the benzyl-protected starting material (1 eq.) was dissolved in tetrahydrofuran or ethyl acetate or methanol or a mixture of tetrahydrofuran and ethyl acetate (1:1) then a catalytic amount of 5% Pd/C catalyst was added. The reaction mixture was put under vacuum followed by hydrogen atmosphere. The mixture was stirred at room temperature until complete consumption of the starting material. The mixture was then filtered through celite, and the solvent was evaporated to give the crude residue which was purified using MPLC. The yields were around 25-90%.

### 3. *In vitro* HDAC inhibitory activity

HDAC1, HDAC6 and HDAC8

The *in vitro* testing on recombinant HDACs were performed as previously described [63] Recombinant human HDAC1 and -6 were purchased from BPS Biosciences. The enzyme inhibition was determined by using a reported homogenous fluorescence assay. [64] The enzymes were incubated for 90 min at 37°C, with the fluorogenic substrate ZMAL (Z-(Ac)Lys-AMC) in a concentration of 10.5 mM and increasing concentrations of inhibitors with subsequent addition of 60 mL of buffer containing trypsin (1 mg/ml) and TSA (2.75 mM) and further incubation for 20 min at 37°C. Fluorescence intensity was measured at an excitation wavelength of 390 nm and an emission wavelength of 460 nm in a microtiter plate reader (BMG Polarstar).

Recombinant hHDAC8 was produced by Romier et al. in Strasbourg. [65] The HDAC8 activity assays were performed according to the commercial HDAC8 Fluorometric Drug Discovery Kit [Fluor de Lys(R)-HDAC8, BML-KI178] corresponding to the manufacturer's instructions. As substrate a tetrapeptide connected to aminomethylcoumarin (AMC) H<sub>2</sub>N-Arg- His-Lys(Ac)-Lys(Ac)-AMC was synthesized as previously described. [63] The enzyme was incubated for 90 min at 37 °C, with a substrate concentration of 50 μM and increasing concentrations of inhibitors. The stop-solution containing inhibitor, to stop the hHDAC8 activity, and Trypsin, to release the AMC, was added. The solution was incubated for 20 min at 37 °C to develop the assay. Fluorescence intensity was measured at an excitation wavelength of 355 nm and an emission wavelength of 460 nm in a microtiter plate reader (BMG Polarstar).

Inhibition was measured at increasing concentration and IC<sub>50</sub> was calculated by nonlinear regression with Origin 9.0G software.

## 4. Cellular testing

### A. Cell culture

Human neuroblastoma cell lines SK-N-BE(2)-C (European Collection of Authenticated Cell Cultures, ECACC, Salisbury, UK) and IMR-32 (German Collection of Microorganisms and Cell Cultures, DSMZ, Darmstadt, Germany) were cultured under standard conditions in Dulbecco's Modified Eagles Medium (DMEM containing L-glutamine and 4.5 g/L glucose, Gibco Invitrogen cell culture, Invitrogen, Paisley, UK) supplemented with 10% fetal calf serum (FCS; Sigma, St. Louis, MO, USA) and 1% non-essential amino acids (NEAA; Invitrogen, Carlsbad, CA, USA). All cell lines were regularly checked for mycoplasma and multiple contaminations (Multiplexion, Heidelberg, Germany) and routinely verified using DNA fingerprinting authentication by Multiplexion.

### B. Western blot

Western blot analysis was performed as described previously (Kolbinger et al.). The following antibodies were used: anti-HDAC8 (H-145) (polyclonal; Santa Cruz, Santa Cruz, CA, USA), anti-HDAC6 (sc-11420, Santa Cruz), anti-HDAC10 (H3413, Sigma), anti-tubulin (#2148, Cell Signaling Technology), anti-acetylated tubulin (#6793, Sigma-Aldrich), anti-acetylated SMC3 (kindly provided by Katsuhiko Shirahige, Institute for Molecular and Cellular Biosciences, University of Tokyo, Japan (Nishiyama et al. 2010)), anti-GAPDH (clone 6C5; Merck) and anti- $\beta$ -actin (#5441, Sigma-Aldrich).

### C. Cell viability assay (Trypan blue assay)

Adherent cells were detached using trypsin–EDTA (ThermoFisher Scientific) and pooled with corresponding supernatant, centrifuged and resuspended in 1 ml of cell culture medium. Cell viability (viable cell number, % viability, % dead cells) was measured by automated trypan blue staining using the Vi-Cell XR Cell Viability Analyzer (Beckman Coulter, Krefeld, Germany).

### D. Colony formation assay

In six-well plates, 500 cells were seeded and treated as indicated. Viable colonies were stained after a minimum of 10 days with crystal violet. For quantification, the mean intensity of each well of the 8-bit binary picture was measured with ImageJ software (U. S. National Institutes of Health, Bethesda, MD, USA; <http://imagej.nih.gov/ij/>).

### E. Cell differentiation assay

Adherent cells plated on 6-well plates were treated as indicated. For staining, cells were rinsed once with (PBS) and incubated with crystal violet staining solution (1% (w/v) in 70% EtOH) for 1 min. Subsequently, the staining solution was removed and cells were rinsed two to three times with autoclaved purified water and allowed to dry. All-trans retinoic acid (ATRA, Sigma-Aldrich, stock concentration 10 mM) was dissolved in ethanol (EtOH, Sigma-Aldrich).

### F. Cytotoxicity studies

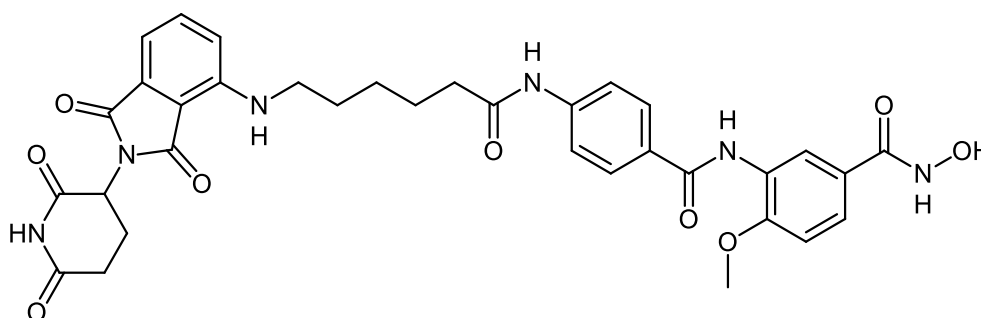
HEK293 cells (DSMZ Braunschweig, ACC305) were incubated at 37 °C in a humidified incubator with 5% CO<sub>2</sub> in Dulbecco's modified Eagle medium (DMEM) supplemented with 10% FCS and 5 mM glutamine. The cells were seeded out at 1.5

× 10<sup>3</sup> cells per well in a 96-well cell culture plate (TPP, Switzerland). All tested compounds were added immediately to the medium at 50 μM or increasing concentrations to determine IC<sub>50</sub> values. After 24 h, Alamar Blue reagent (Invitrogen, CA) was added according to the manufacturer's instructions and incubated again for 21 h before the samples were analyzed. Detection of the viable cells which convert the resazurine of reagent into the high fluorescent resorufin was performed by using a FLUOstar OPTIMA microplate reader (BMG Labtec) with the following filter set: Ex 560 nm/Em 590 nm.

The measurements were performed in triplicate, and data are the mean with SD ≤ 12%. As a positive control daunorubicin was used, and an IC<sub>50</sub> value of 12.55 ± 0.07 μM was obtained.

## 5. Characterization data of the final compounds

### 3-(4-(6-((2-(2,6-Dioxopiperidin-3-yl)-1,3-dioxoisindolin-4-yl)amino)hexanamido)benzamido)-*N*-hydroxy-4-methoxybenzamide (1a)



MS m/z: 669.34 [M-H]<sup>-</sup>

<sup>1</sup>H NMR (400 MHz, DMSO-d<sub>6</sub>) δ 11.06 (s, 2H), 10.14 (s, 1H), 9.36 (s, 1H), 8.18 (d, *J* = 2.1 Hz, 1H), 7.90 (d, *J* = 8.8 Hz, 2H), 7.71 (d, *J* = 8.7 Hz, 2H), 7.62 – 7.52 (m, 2H), 7.12 (d, *J* = 8.7 Hz, 1H), 7.09 (d, *J* = 8.6 Hz, 1H), 7.00 (d, *J* = 7.0 Hz, 1H), 6.53 (t, *J* =

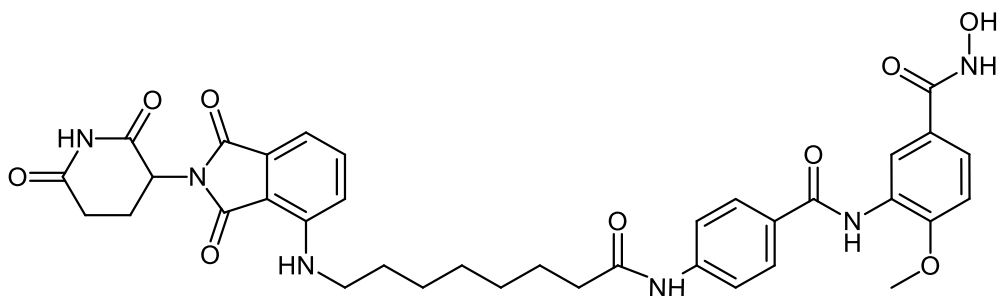
5.9 Hz, 1H), 5.03 (dd,  $J = 12.8, 5.4$  Hz, 1H), 3.86 (s, 3H), 2.94 – 2.78 (m, 2H), 2.68 – 2.51 (m, 2H), 2.35 (t,  $J = 7.3$  Hz, 2H), 2.09 – 1.90 (m, 2H), 1.63 (tt,  $J = 15.0, 7.3$  Hz, 4H), 1.45 – 1.32 (m, 2H).

$^{13}\text{C}$  NMR (101 MHz, DMSO- $d_6$ )  $\delta$  173.34, 172.28, 170.55, 169.38, 167.78, 165.05, 154.29, 146.87, 142.77, 136.79, 132.55, 128.86, 128.76, 127.04, 118.82, 118.53, 111.33, 110.89, 109.37, 56.47, 51.59, 49.03, 48.97, 36.81, 31.37, 28.91, 26.37, 25.17, 22.58.

HRMS: 693.227  $[\text{M}+\text{Na}]^+$ , calculated  $\text{C}_{34}\text{H}_{34}\text{N}_6\text{O}_9\text{Na}^+$ : 693.228

HPLC: (M2) rt. 9.7 min (purity >99%)

**3-(4-(8-((2-(2,6-Dioxopiperidin-3-yl)-1,3-dioxoisindolin-4-yl)amino)octanamido)benzamido)-*N*-hydroxy-4-methoxybenzamide (1b)**



MS  $m/z$ : 697.62  $[\text{M}-\text{H}]^-$

$^1\text{H}$  NMR (400 MHz, DMSO- $d_6$ )  $\delta$  11.05 (s, 2H), 10.14 (s, 1H), 9.36 (s, 1H), 8.17 (d,  $J = 1.7$  Hz, 1H), 7.90 (d,  $J = 8.7$  Hz, 2H), 7.71 (d,  $J = 8.5$  Hz, 2H), 7.64 – 7.49 (m, 2H), 7.12 (d,  $J = 8.7$  Hz, 1H), 7.07 (d,  $J = 8.6$  Hz, 1H), 7.00 (d,  $J = 7.0$  Hz, 1H), 6.51 (t,  $J = 5.5$  Hz, 1H), 5.03 (dd,  $J = 12.9, 5.2$  Hz, 1H), 3.86 (s, 3H), 2.95 – 2.75 (m, 2H), 2.67 – 2.52 (m, 2H), 2.39 – 2.27 (m, 2H), 2.09 – 1.92 (m, 2H), 1.68 – 1.47 (m, 4H), 1.40 – 1.23 (m, 6H).

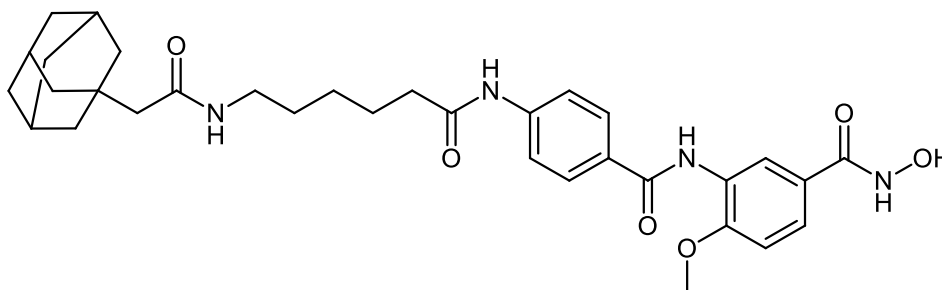


$^{13}\text{C}$  NMR (101 MHz, DMSO- $d_6$ )  $\delta$  173.25, 172.24, 170.52, 167.75, 164.94, 146.88, 142.84, 136.74, 132.61, 128.87, 118.74, 110.83, 109.43, 72.91, 63.51, 56.48, 48.99, 36.78, 31.41, 29.09, 29.04, 28.94, 26.63, 25.37.

HRMS: 699.279  $[\text{M}+\text{H}]^+$ , calculated  $\text{C}_{36}\text{H}_{39}\text{N}_6\text{O}_9^+$ : 699.278

HPLC: (M2) rt. 10.3 min (purity 99%)

**3-(4-(6-(2-(Adamantan-1-yl)acetamido)hexanamido)benzamido)-*N*-hydroxy-4-methoxybenzamide (1m)**



MS  $m/z$ : 589.45  $[\text{M}-\text{H}]^-$

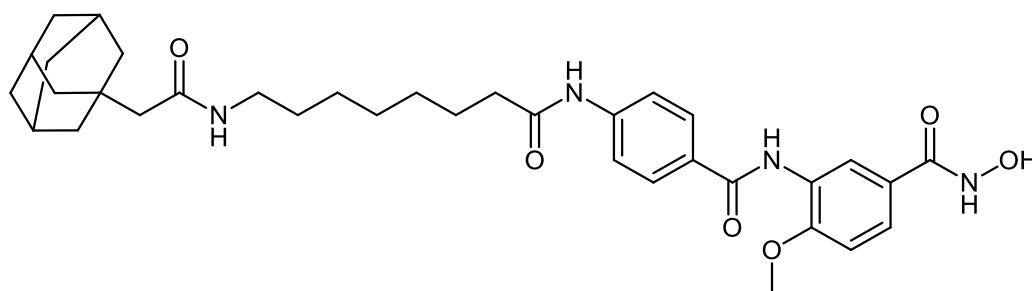
$^1\text{H}$  NMR (400 MHz, DMSO- $d_6$ )  $\delta$  11.05 (s, 2H), 10.14 (s, 1H), 9.36 (s, 1H), 8.18 (d,  $J = 2.1$  Hz, 1H), 7.91 (d,  $J = 8.7$  Hz, 2H), 7.71 (d,  $J = 8.7$  Hz, 2H), 7.67 – 7.55 (m, 2H), 7.12 (d,  $J = 8.7$  Hz, 1H), 3.87 (s, 3H), 3.00 (dd,  $J = 12.6, 6.6$  Hz, 2H), 2.33 (t,  $J = 7.3$  Hz, 2H), 1.94 – 1.84 (m, 3H), 1.79 (s, 2H), 1.69 – 1.47 (m, 14H), 1.46 – 1.35 (m, 2H), 1.35 – 1.24 (m, 2H).

$^{13}\text{C}$  NMR (101 MHz, DMSO- $d_6$ )  $\delta$  172.18, 170.29, 164.96, 154.26, 142.83, 128.84, 128.74, 127.10, 125.11, 124.86, 123.93, 118.76, 118.39, 111.31, 56.47, 50.54, 49.08, 39.23, 38.64, 36.90, 32.57, 29.42, 28.47, 26.58, 25.13.

HRMS: 591.319  $[\text{M}+\text{H}]^+$ , calculated  $\text{C}_{33}\text{H}_{43}\text{N}_4\text{O}_6^+$ : 591.318

HPLC: (M2) rt. 10.5 min (purity 93 %)

**3-(4-(8-(2-(Adamantan-1-yl)acetamido)octanamido)benzamido)-*N*-hydroxy-4-methoxybenzamide (1n)**



MS m/z: 617.60 [M-H]<sup>-</sup>

<sup>1</sup>H NMR (400 MHz, DMSO-d<sub>6</sub>) δ 11.02 (s, 2H), 10.13 (s, 1H), 9.35 (s, 1H), 8.17 (d, J = 2.1 Hz, 1H), 7.90 (d, J = 8.8 Hz, 2H), 7.71 (d, J = 8.8 Hz, 2H), 7.58 (dd, J = 8.5, 2.2 Hz, 2H), 7.11 (d, J = 8.7 Hz, 1H), 3.86 (s, 3H), 2.99 (dd, J = 12.6, 6.6 Hz, 2H), 2.32 (t, J = 7.4 Hz, 2H), 1.93 – 1.82 (m, 3H), 1.78 (s, 2H), 1.74 – 1.42 (m, 14H), 1.41 – 1.16 (m, 8H).

<sup>13</sup>C NMR (101 MHz, DMSO-d<sub>6</sub>) δ 172.16, 170.09, 164.89, 154.19, 142.87, 128.85, 128.74, 127.14, 125.22, 124.88, 123.97, 118.71, 118.40, 111.28, 56.48, 50.56, 38.64, 36.92, 32.58, 29.61, 29.10, 28.95, 28.49, 26.77, 25.40.

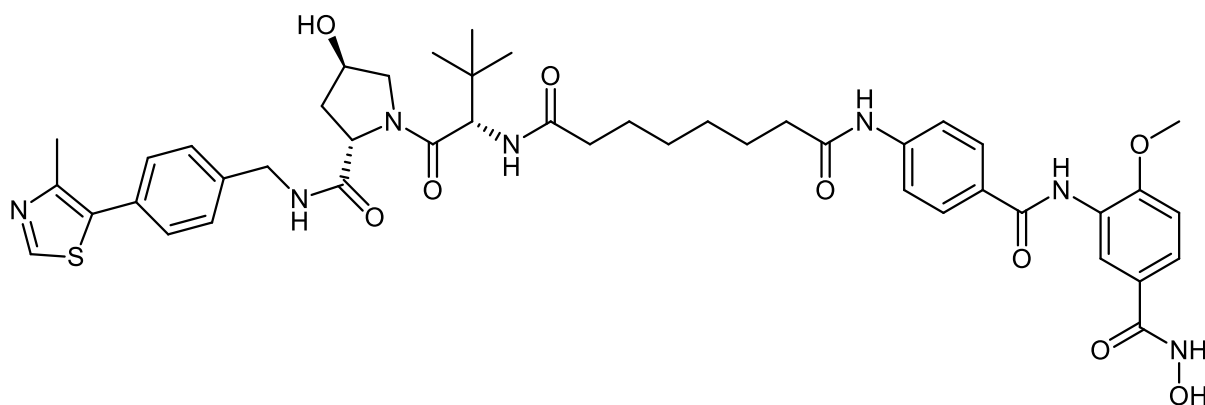
HRMS: 619.350 [M+H]<sup>+</sup>, calculated C<sub>35</sub>H<sub>47</sub>N<sub>4</sub>O<sub>6</sub><sup>+</sup>: 619.350

HPLC: (M2) rt. 14.2 min (purity > 99 %)

The synthesis of the PROTACs (**1a**, **1b**, **1m** and **1n**) is elucidated in **scheme 1**. After 4-((tert-butoxycarbonyl) amino)benzoic acid (**4**) was prepared as previously reported [66], it was reacted with methyl 3-amino-4-methoxybenzoate (**6a**) following method IIIA to yield methyl 3-(4-((tert-butoxycarbonyl)amino)benzamido)-4-methoxybenzoate (**7**). Next, the methyl ester group was hydrolysed using the general method IIA and

the tert-butyloxycarbonyl protecting group was removed using method VI to yield 3-(4-aminobenzamido)-4-methoxybenzoic acid (**8**). To complete the synthesis of the 2-tetrahydropyranyl-protected HDAC ligand (**9**), *O*-(tetrahydro-2*H*-pyran-2-yl) hydroxylamine was reacted with the free carboxylic group following method IIIA. The 2-tetrahydropyranyl protected PROTACs were synthesised by reacting the different E3 ligase ligand-linker-COOH (**43a,b**) or HyT-linker-COOH (**47a,b**) (see synthesis in Supp. Info.) with the 2-tetrahydropyranyl-protected HDAC ligand (**9**) as stated in the general method IIIA. Finally, deprotection according to the general method V took place to obtain the free hydroxamic acid containing PROTACs (**1a**, **1b**, **1m** and **1n**).

***N*<sup>1</sup>-((*S*)-1-((2*S*,4*R*)-4-hydroxy-2-((4-(4-methylthiazol-5-yl)benzyl)carbamoyl)pyrrolidin-1-yl)-3,3-dimethyl-1-oxobutan-2-yl)-*N*<sup>8</sup>-(4-((5-(hydroxycarbamoyl)-2-methoxyphenyl) carbamoyl) phenyl)octanediamide (**1k**)**



MS *m/z*: 868.41 [*M*-*H*]<sup>-</sup>

<sup>1</sup>H NMR (400 MHz, DMSO-*d*<sub>6</sub>) δ 11.08 (s, 2H), 10.14 (s, 1H), 9.37 (s, 1H), 8.96 (s, 1H), 8.53 (t, *J* = 6.0 Hz, 1H), 8.17 (d, *J* = 2.1 Hz, 1H), 7.91 (d, *J* = 8.8 Hz, 2H), 7.82 (d, *J* = 9.3 Hz, 1H), 7.71 (d, *J* = 8.8 Hz, 2H), 7.59 (dd, *J* = 8.6, 2.2 Hz, 1H), 7.46 – 7.29 (m, 3H), 7.12 (d, *J* = 8.7 Hz, 1H), 5.11 (s, 1H), 4.53 (d, *J* = 9.4 Hz, 1H), 4.46 – 4.29 (m, 3H), 4.20 (dd, *J* = 15.9, 5.5 Hz, 1H), 3.86 (s, 3H), 3.70 – 3.52 (m, 2H), 2.43

(s, 3H), 2.29 – 1.94 (m, 4H), 1.64 – 1.39 (m, 4H), 1.34 – 1.20 (m, 4H), 0.92 (s,  $J = 7.9$  Hz, 9H).

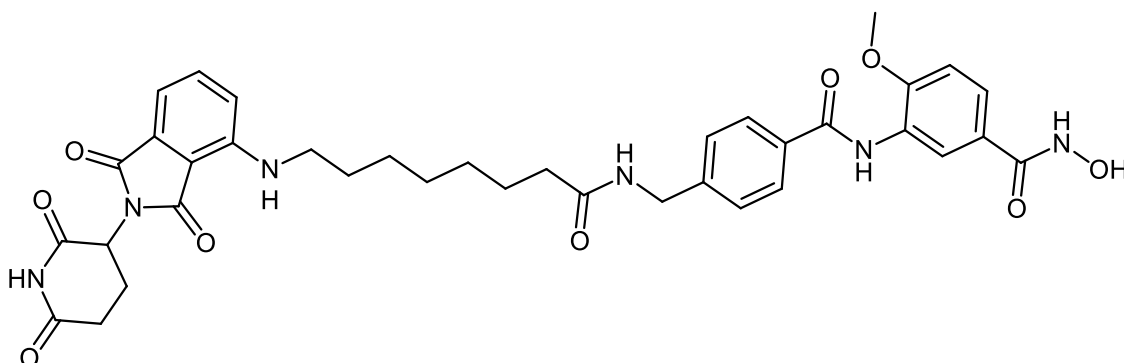
$^{13}\text{C}$  NMR (101 MHz, DMSO- $d_6$ )  $\delta$  173.09, 172.69, 172.68, 172.43, 172.29, 170.17, 164.99, 154.27, 151.89, 148.13, 142.82, 139.88, 131.61, 130.05, 129.07, 128.86, 128.74, 127.86, 127.10, 127.08, 125.07, 118.78, 118.77, 118.52, 111.32, 69.31, 59.15, 56.80, 56.77, 56.47, 49.03, 38.33, 35.63, 35.32, 28.89, 28.84, 26.80, 25.77, 25.35, 16.33.

HRMS: 870.388  $[\text{M}+\text{H}]^+$ , calculated  $\text{C}_{45}\text{H}_{56}\text{N}_7\text{O}_9\text{S}^+$  870.386

HPLC: (M2) rt. 9.9 min (purity 96%)

In **scheme 2**, the synthesis of PROTAC (**1k**) is shown. First, the 2-tetrahydropyranyl-protected HDAC ligand (**9**) was synthesized as previously indicated in **scheme 1**. Next, suberic acid was attached to the protected ligand following method IIID to yield 8-((4-((2-methoxy-5-(((tetrahydro-2*H*-pyran-2-yl)oxy)carbamoyl)phenyl)carbamoyl)phenyl)amino)-8-oxooctanoic acid (**10**). Then the formed conjugate was reacted with the VHL ligand (**40**) using method IIIA to give the protected PROTAC which was deprotected according to method V.

**3-(4-((8-((2-(2,6-Dioxopiperidin-3-yl)-1,3-dioxoisindolin-4-yl)amino)octanamido)methyl)benzamido)-*N*-hydroxy-4-methoxybenzamide (1c)**



MS m/z: 711.36 [M-H]<sup>-</sup>

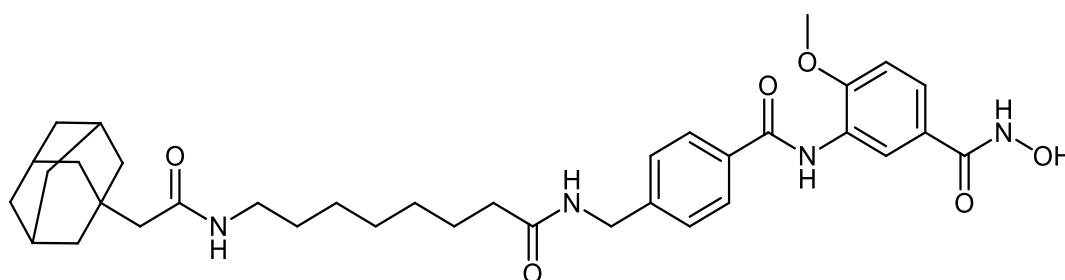
<sup>1</sup>H NMR (400 MHz, DMSO-d<sub>6</sub>) δ 11.04 (s, 2H), 9.45 (s, 1H), 8.35 (t, *J* = 5.9 Hz, 1H), 8.17 (d, *J* = 2.1 Hz, 1H), 7.90 (d, *J* = 8.2 Hz, 2H), 7.66 – 7.50 (m, 2H), 7.35 (d, *J* = 8.2 Hz, 2H), 7.12 (d, *J* = 8.7 Hz, 1H), 7.07 (d, *J* = 8.6 Hz, 1H), 6.99 (d, *J* = 7.0 Hz, 1H), 6.50 (t, *J* = 5.7 Hz, 1H), 5.02 (dd, *J* = 12.8, 5.4 Hz, 1H), 4.31 (d, *J* = 5.8 Hz, 2H), 3.85 (s, 3H), 3.00 – 2.73 (m, 2H), 2.69 – 2.51 (m, 2H), 2.14 (t, *J* = 7.4 Hz, 2H), 2.07 – 1.86 (m, 2H), 1.67 – 1.40 (m, 4H), 1.40 – 1.14 (m, 6H).

<sup>13</sup>C NMR (101 MHz, DMSO-d<sub>6</sub>) δ 173.22, 172.71, 170.52, 169.39, 167.73, 165.30, 154.32, 146.87, 144.20, 136.71, 133.15, 132.63, 127.98, 127.54, 127.01, 125.17, 125.06, 124.14, 117.61, 111.34, 110.81, 109.46, 56.48, 49.04, 48.99, 42.27, 35.76, 31.42, 29.08, 28.92, 26.67, 25.68, 22.59.

HRMS: 713.295 [M+H]<sup>+</sup>, calculated C<sub>37</sub>H<sub>41</sub>N<sub>6</sub>O<sub>9</sub><sup>+</sup>: 713.294

HPLC: (M2) rt. 12.2 min (purity >99 %)

**3-(4-((8-(2-(Adamantan-1-yl)acetamido)octanamido)methyl)benzamido)-*N*-hydroxy-4-methoxybenzamide (1o)**



MS m/z: 631.54 [M-H]<sup>-</sup>

<sup>1</sup>H NMR (400 MHz, DMSO-d<sub>6</sub>) δ 10.82 (s, 2H), 9.45 (s, 1H), 8.36 (t, *J* = 5.9 Hz, 1H), 8.16 (d, *J* = 2.1 Hz, 1H), 7.90 (d, *J* = 8.3 Hz, 2H), 7.70 – 7.51 (m, 2H), 7.35 (d, *J* = 8.3

Hz, 2H), 7.12 (d,  $J = 8.7$  Hz, 1H), 4.31 (d,  $J = 5.9$  Hz, 2H), 3.85 (s, 3H), 2.99 (dd,  $J = 12.6, 6.7$  Hz, 2H), 2.13 (t,  $J = 7.4$  Hz, 2H), 1.94 – 1.83 (m, 3H), 1.78 (s, 2H), 1.73 – 1.42 (m, 12H), 1.43 – 1.30 (m, 2H), 1.29 – 1.12 (m, 8H).

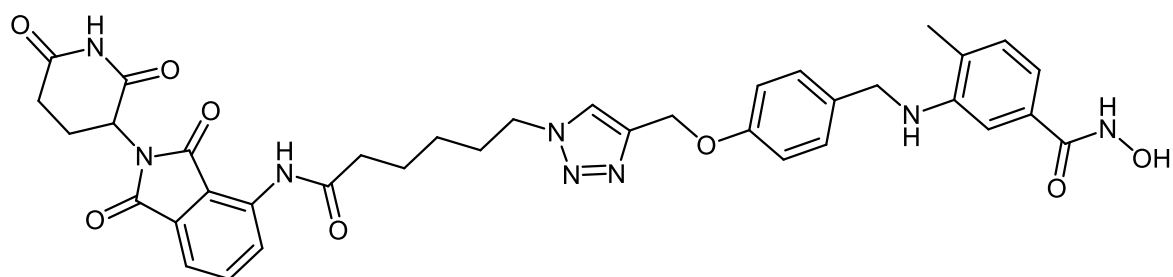
$^{13}\text{C}$  NMR (101 MHz, DMSO- $d_6$ )  $\delta$  172.68, 170.10, 165.29, 154.31, 144.19, 133.16, 127.98, 127.76, 127.55, 127.51, 127.00, 125.27, 124.18, 111.33, 56.48, 50.54, 42.59, 36.92, 35.78, 32.58, 29.62, 29.13, 28.90, 28.49, 26.80, 25.68.

HRMS: 633.366  $[\text{M}+\text{H}]^+$ , calculated  $\text{C}_{36}\text{H}_{49}\text{N}_4\text{O}_6^+$ : 633.365

HPLC: (M2) rt. 13.8 min (purity 99%)

According to the general method IIIB compound 3-(4-(((tert-butoxycarbonyl)amino)methyl) benzamido)-4-methoxybenzoic acid (**13**) was synthesized starting from 4-(((tert-butoxycarbonyl)amino)methyl)benzoic acid (**11**) and methyl 3-amino-4-methoxybenzoate (**6a**). Tert-butyl (4-(chlorocarbonyl) benzyl)carbamate (**12**) was prepared in accordance to a previously reported method [67]. The methyl ester was hydrolysed according to method IIA to obtain the free carboxylic acid which was reacted with *O*-benzylhydroxylamine hydrochloride according to method IIIA to give the benzyl protected HDAC ligand (**14**). Next, the tert-butyloxycarbonyl protecting group was removed using method VI. The PROTAC synthesis was completed by reacting the E3 ligase ligand-linker-COOH (**43b**) or HyT-linker-COOH (**47b**) with the protected HDAC ligand (**14**) using method IIIA followed by removing the benzyl group according to the method VII to obtain the free hydroxamic acid. The synthesis of the PROTACs (**1c** and **1o**) is shown in **scheme 3**.

**3-(((4-(((1-(6-((2-(2,6-Dioxopiperidin-3-yl)-1,3-dioxoisindolin-4-yl)amino)-6-oxohexyl)-1*H*-1,2,3-triazol-4-yl)methoxy)benzyl)amino)-*N*-hydroxy-4-methylbenzamide (**1d**)**



MS m/z: 721.67 [M-H]<sup>-</sup>

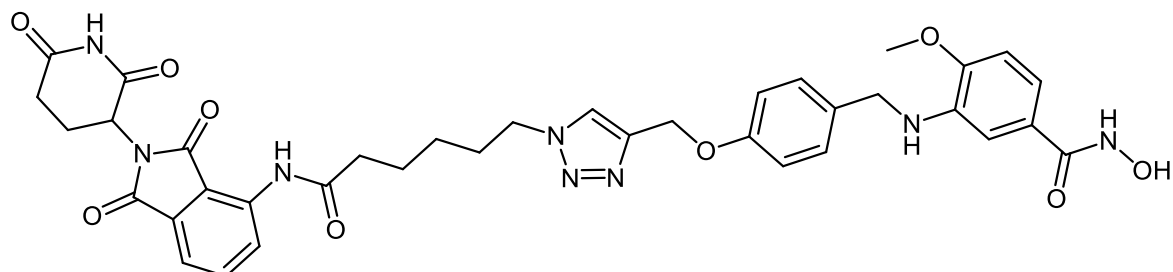
<sup>1</sup>H NMR (400 MHz, DMSO-d<sub>6</sub>) δ 11.11 (s, 1H), 10.88 (s, 1H), 9.67 (s, 1H), 8.75 (d, J = 1.7 Hz, 1H), 8.44 (d, J = 8.5 Hz, 1H), 8.18 (s, 1H), 7.83 – 7.77 (m, 1H), 7.59 (d, J = 7.2 Hz, 1H), 7.26 (d, J = 8.5 Hz, 2H), 7.00 – 6.92 (m, 3H), 6.86 – 6.80 (m, 2H), 5.61 (t, J = 5.9 Hz, 1H), 5.12 (dd, J = 12.7, 5.3 Hz, 1H), 5.06 (s, 2H), 4.38 – 4.27 (m, 4H), 2.92 – 2.81 (m, 1H), 2.63 – 2.51 (m, 2H), 2.45 – 2.41 (m, 1H), 2.14 (s, 3H), 1.89 – 1.78 (m, 2H), 1.69 – 1.58 (m, 2H), 1.57 – 1.46 (m, 2H), 1.33 – 1.26 (m, 2H).

<sup>13</sup>C NMR (101 MHz, cd<sub>3</sub>od) δ 172.46, 172.32, 169.06, 168.96, 166.88, 157.41, 146.20, 143.85, 137.12, 136.23, 131.91, 131.21, 130.44, 129.87, 128.76, 126.17, 125.23, 123.31, 118.50, 115.28, 114.91, 108.24, 77.50, 61.64, 50.09, 49.28, 37.12, 31.18, 29.72, 25.71, 24.29, 22.49, 17.23.

HRMS: 723.290 [M+H]<sup>+</sup>, calculated C<sub>37</sub>H<sub>39</sub>N<sub>8</sub>O<sub>8</sub><sup>+</sup> 723.289

HPLC: (M2) rt: 7.3 min (purity 96 %)

**3-((4-((1-(6-((2-(2,6-Dioxopiperidin-3-yl)-1,3-dioxoisindolin-4-yl)amino)-6-oxohexyl)-1*H*-1,2,3-triazol-4-yl)methoxy)benzyl)amino)-*N*-hydroxy-4-methoxybenzamide (1e)**



MS m/z: 737.62 [M-H]<sup>-</sup>

<sup>1</sup>H NMR (400 MHz, DMSO-d<sub>6</sub>) δ 11.10 (s, 1H), 10.87 (s, 1H), 9.67 (s, 1H), 8.72 (s, 4H), 8.44 (d, J = 8.4 Hz, 1H), 8.18 (s, 1H), 7.80 (t, J = 7.9 Hz, 1H), 7.59 (d, J = 7.3 Hz, 1H), 7.24 (d, J = 8.5 Hz, 2H), 6.98 (d, J = 1.6 Hz, 1H), 6.94 (d, J = 8.8 Hz, 2H), 6.86 (d, J = 1.3 Hz, 1H), 6.81 (d, J = 8.3 Hz, 1H), 5.48 (t, J = 6.0 Hz, 1H), 5.12 (dd, J = 12.7, 5.4 Hz, 1H), 5.06 (s, 2H), 4.34 (t, J = 7.1 Hz, 2H), 4.26 (d, J = 6.1 Hz, 2H), 3.81 (s, 3H), 2.67 – 2.51 (m, 2H), 2.46 – 2.34 (m, 2H), 2.13 – 2.00 (m, 1H), 1.91 – 1.78 (m, 2H), 1.70 – 1.58 (m, 2H), 1.53 – 1.40 (m, 1H), 1.37 – 1.25 (m, 2H).

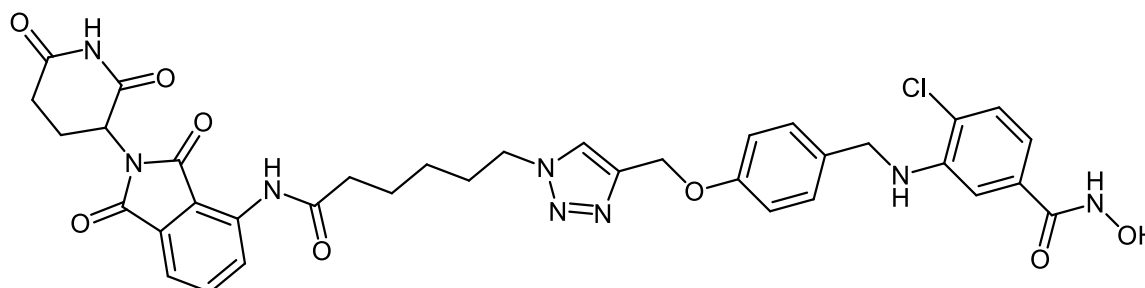
<sup>13</sup>C NMR (101 MHz, DMSO-d<sub>6</sub>) δ 173.17, 172.30, 170.20, 168.08, 167.09, 157.38, 149.04, 143.13, 137.88, 136.94, 136.51, 132.64, 131.90, 128.72, 126.78, 125.74, 124.73, 118.75, 117.48, 114.97, 109.33, 61.61, 55.99, 49.66, 49.36, 45.93, 36.62, 31.37, 29.85, 25.78, 24.55, 22.43.

HRMS: 739.284 [M+H]<sup>+</sup>, calculated C<sub>37</sub>H<sub>39</sub>N<sub>8</sub>O<sub>9</sub><sup>+</sup> 739.284

HPLC: (M2) rt: 10.9 min (purity 99 %)



**4-Chloro-3-((4-((1-(6-((2-(2,6-dioxopiperidin-3-yl)-1,3-dioxoisindolin-4-yl)amino)-6-oxohexyl)-1*H*-1,2,3-triazol-4-yl)methoxy)benzyl)amino)-*N*-hydroxybenzamide (1f)**



MS m/z: 741.59 [M-H]<sup>-</sup>

<sup>1</sup>H NMR (400 MHz, DMSO-d<sub>6</sub>) δ 11.11 (s, 2H), 9.67 (s, 1H), 8.94 (s, 1H), 8.44 (d, J = 8.4 Hz, 1H), 8.18 (s, 1H), 7.84 – 7.75 (m, 1H), 7.58 (d, J = 7.2 Hz, 1H), 7.32 – 7.21 (m, 3H), 7.00 – 6.93 (m, 3H), 6.90 (dd, J = 8.2, 1.8 Hz, 1H), 6.13 (t, J = 5.9 Hz, 1H), 5.12 (dd, J = 12.8, 5.4 Hz, 1H), 5.06 (s, 2H), 4.41 – 4.29 (m, 4H), 2.65 – 2.50 (m, 2H), 2.47 – 2.37 (m, 2H), 2.30 – 2.20 (m, 1H), 1.90 – 1.75 (m, 2H), 1.70 – 1.59 (m, 2H), 1.56 – 1.46 (m, 1H), 1.36 – 1.24 (m, 2H).

<sup>13</sup>C NMR (101 MHz, DMSO-d<sub>6</sub>) δ 173.17, 172.30, 170.20, 168.09, 167.09, 157.44, 144.23, 143.10, 136.94, 136.51, 132.82, 132.00, 131.90, 129.25, 128.49, 126.79, 124.74, 120.84, 118.75, 117.48, 115.05, 110.31, 61.60, 49.66, 49.36, 45.70, 36.63, 31.37, 29.85, 25.79, 24.55, 22.44.

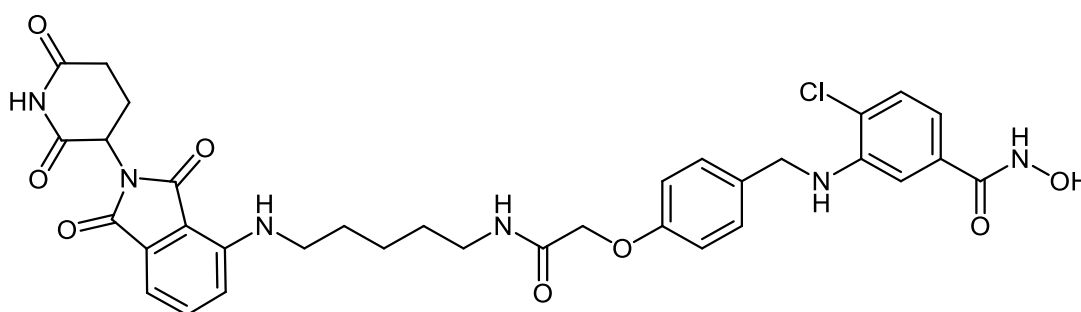
HRMS: 743.235 [M+H]<sup>+</sup>, calculated C<sub>36</sub>H<sub>36</sub>ClN<sub>8</sub>O<sub>8</sub><sup>+</sup> 743.234

HPLC: (M1) rt: 12.9 min (purity 97 %)

To prepare 4-substituted-3-[[4-(proparg-1-yloxy)benzyl]amino]benzoic acid (**17a-c**), 4-proparg-1-yloxybenzaldehyde (**16**) and the corresponding amine (**5 a-c**) were

reacted according to the method IA. Afterwards, the 2-tetrahydropyranyl-protected HDAC ligand were prepared by reacting the free carboxylic acid in (**17a-c**) with *O*-(tetrahydro-2*H*-pyran-2-yl)hydroxylamine following the general method IIIA. Next, these HDAC ligands (**18a-c**) were linked to the E3 ligase ligand-linker-N<sub>3</sub> (**50**) via the azide-alkyne Huisgen cycloaddition as stated in method IV. Finally, the free hydroxamic acid was obtained by removing the 2-tetrahydropyranyl group following method V. The synthesis of these PROTACs (**1d-f**) is presented in **scheme 4**.

**4-Chloro-3-[(4-{2-[(5-{[2-(2,6-dioxopiperidin-3-yl)-1,3-dioxoisindolin-4-yl]amino}pentyl)amino]-2-oxoethoxy}benzyl)amino]-*N*-hydroxybenzamide (1g)**



MS m/z: 689.24 [M-H]<sup>-</sup>

<sup>1</sup>H NMR (400 MHz, DMSO-d<sup>6</sup>) δ 11.06 (s, 2H), 8.93 (s, 1H), 8.01 (t, J = 5.7 Hz, 1H), 7.59 – 7.51 (m, 1H), 7.31 – 7.19 (m, 3H), 7.06 (d, J = 8.6 Hz, 1H), 7.00 (d, J = 7.0 Hz, 1H), 6.96 – 6.83 (m, 4H), 6.49 (t, J = 5.7 Hz, 1H), 6.14 (t, J = 6.1 Hz, 1H), 5.03 (dd, J = 12.9, 5.3 Hz, 1H), 4.40 (s, 2H), 4.35 (d, J = 6.0 Hz, 2H), 3.25 (dd, J = 13.5, 6.8 Hz, 2H), 3.11 (dd, J = 13.0, 6.6 Hz, 2H), 2.92 – 2.79 (m, 1H), 2.60 – 2.52 (m, 2H), 2.04 – 1.96 (m, 1H), 1.58 – 1.40 (m, 4H), 1.34 – 1.24 (m, 2H).

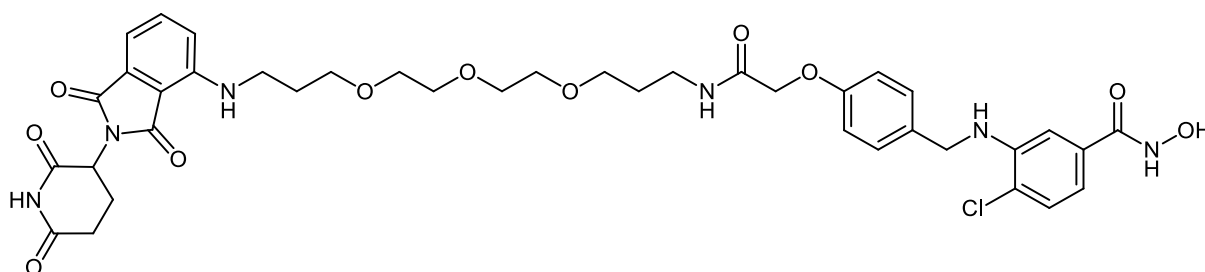
<sup>13</sup>C NMR (101 MHz, DMSO-d<sup>6</sup>) δ 173.21, 170.51, 169.38, 167.91, 167.73, 164.34, 157.10, 146.85, 144.21, 136.71, 132.81, 132.63, 132.37, 129.25, 128.42, 120.85,

117.61, 115.21, 115.11, 110.83, 110.29, 109.48, 79.61, 67.53, 49.00, 45.70, 42.24, 38.56, 31.43, 30.83, 29.21, 28.78, 24.06, 22.61.

HRMS m/z: 691.229 [M+H]<sup>+</sup>, calculated C<sub>34</sub>H<sub>36</sub>ClN<sub>6</sub>O<sub>8</sub><sup>+</sup>: 691.228

HPLC: (M2) rt 9.5 min (purity 98 %)

**4-Chloro-3-({4-[(16-{{2-(2,6-dioxopiperidin-3-yl)-1,3-dioxoisindolin-4-yl}amino)-2-oxo-7,10,13-trioxa-3-azahexadecyl]oxy]benzyl}amino)-N-hydroxybenzamide  
(1h)**



MS m/z: 807.53 [M-H]<sup>-</sup>

<sup>1</sup>H NMR (400 MHz, DMSO-d<sup>6</sup>) δ 11.05 (s, 2H), 8.92 (s, 1H), 7.97 (t, J = 5.7 Hz, 1H), 7.55 (dd, J = 8.4, 7.2 Hz, 1H), 7.30 – 7.20 (m, 3H), 7.07 (d, J = 8.6 Hz, 1H), 6.99 (d, J = 6.9 Hz, 1H), 6.94 (d, J = 1.9 Hz, 1H), 6.91 – 6.85 (m, 3H), 6.63 (t, J = 5.9 Hz, 1H), 6.14 (t, J = 6.1 Hz, 1H), 5.02 (dd, J = 12.8, 5.4 Hz, 1H), 4.39 (s, 2H), 4.35 (d, J = 6.1 Hz, 2H), 3.55 – 3.39 (m, 10H), 3.40 – 3.29 (m, 4H), 3.14 (dd, J = 12.9, 6.7 Hz, 2H), 2.92 – 2.79 (m, 1H), 2.66 – 2.52 (m, 2H), 2.04 – 1.95 (m, 1H), 1.82 – 1.73 (m, 2H), 1.67 – 1.56 (m, 2H).

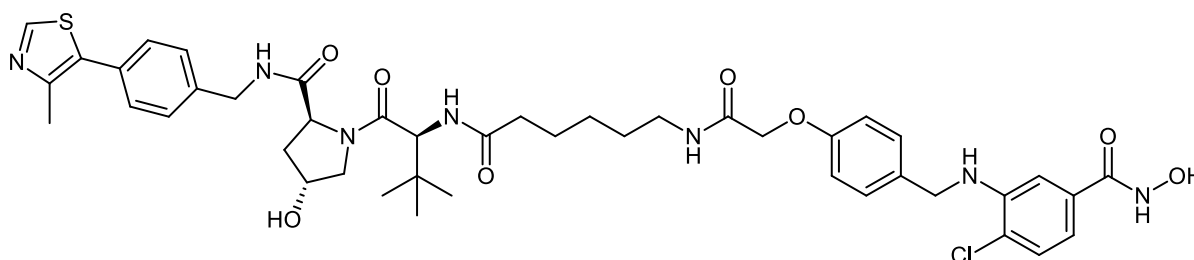
<sup>13</sup>C NMR (101 MHz, DMSO-d<sup>6</sup>) δ 173.22, 170.50, 169.27, 167.84, 167.77, 157.06, 146.88, 144.21, 136.70, 132.83, 132.64, 132.40, 129.25, 128.42, 117.52, 115.22,

115.15, 110.81, 110.28, 110.52, 70.22, 70.17, 70.13, 69.99, 68.65, 67.52, 48.98, 45.69, 36.30, 31.42, 29.69, 29.32, 22.61.

HRMS m/z: 809.292 [M+H]<sup>+</sup>, calculated C<sub>39</sub>H<sub>46</sub>ClN<sub>6</sub>O<sub>11</sub><sup>+</sup> 809.291

HPLC: (M2) rt 9.8 min (purity >99 %)

**(2*S*,4*R*)-1-[(*S*)-2-(6-{2-[4-({[2-chloro-5-(hydroxycarbonyl)phenyl] amino)methyl]phenoxy]acetamido}hexanamido)-3,3-dimethylbutanoyl]-4-hydroxy-*N*-[4-(4-methylthiazol-5-yl)benzyl]pyrrolidine-2-carboxamide (1I)**



MS m/z: 874.38 [M-H]<sup>-</sup>

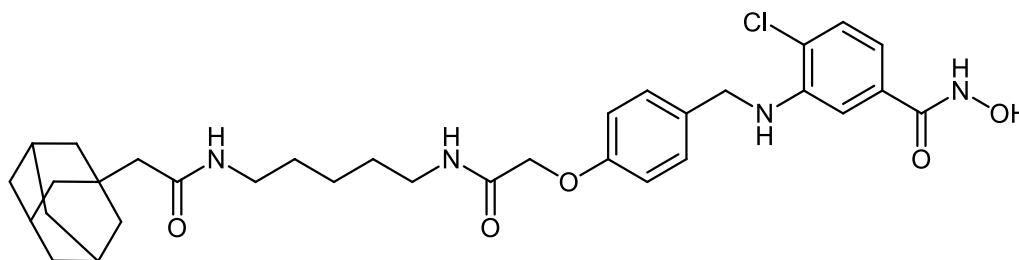
<sup>1</sup>H NMR (400 MHz, DMSO-d<sub>6</sub>) δ 11.06 (s, 1H), 9.00 (s, 1H), 8.54 (t, J = 6.0 Hz, 1H), 7.99 (t, J = 5.8 Hz, 1H), 7.81 (d, J = 9.4 Hz, 1H), 7.43 – 7.33 (m, 4H), 7.30 – 7.20 (m, 3H), 6.96 – 6.85 (m, 4H), 4.52 (d, J = 9.3 Hz, 1H), 4.43 – 4.29 (m, 6H), 3.69 – 3.52 (m, 3H), 3.07 (dd, J = 13.2, 6.7 Hz, 2H), 2.43 (s, 3H), 2.26 – 2.16 (m, 1H), 2.11 – 1.98 (m, 2H), 1.93 – 1.83 (m, 1H), 1.77 – 1.71 (m, 1H), 1.52 – 1.32 (m, 4H), 1.25 – 1.15 (m, 3H), 0.91 (s, 9H).

<sup>13</sup>C NMR (101 MHz, DMSO-d<sub>6</sub>) δ 172.48, 172.37, 170.14, 167.83, 164.28, 157.10, 152.05, 147.87, 144.20, 140.02, 132.36, 129.94, 129.25, 129.08, 128.41, 127.87, 120.84, 115.24, 115.11, 110.31, 79.63, 69.30, 67.51, 59.13, 56.74, 38.63, 38.39, 35.65, 35.29, 29.29, 26.83, 26.50, 25.61, 16.26.

HRMS m/z: 876.353 [M+H]<sup>+</sup>, calculated C<sub>44</sub>H<sub>55</sub>ClN<sub>7</sub>O<sub>8</sub>S<sup>+</sup>: 876.352

HPLC: (M2) rt. 10.2 min (purity 96%)

**3-({4-[2-({5-[2-(Adamantan-1-yl)acetamido]pentyl)amino]-2-oxoethoxy]benzyl}amino)-4-chloro-*N*-hydroxybenzamide (1p)**



MS m/z: 609.65 [M-H]<sup>-</sup>

<sup>1</sup>H NMR (400 MHz, DMSO-d<sub>6</sub>) δ 11.05 (s, 1H), 8.91 (s, 1H), 7.98 (t, J = 5.8 Hz, 1H), 7.59 (s, 1H), 7.30 – 7.21 (m, 3H), 6.96 – 6.84 (m, 4H), 6.15 (t, J = 6.0 Hz, 1H), 4.39 (s, 2H), 4.36 (d, J = 6.1 Hz, 2H), 3.15 (d, J = 5.3 Hz, 1H), 3.08 (dd, J = 13.1, 6.6 Hz, 2H), 2.96 (dd, J = 12.8, 6.7 Hz, 2H), 1.88 (s, 3H), 1.78 (s, 2H), 1.66 – 1.49 (m, 11H), 1.42 – 1.30 (m, 4H), 1.25 – 1.15 (m, 2H).

<sup>13</sup>C NMR (101 MHz, DMSO-d<sub>6</sub>) δ 170.13, 167.85, 164.35, 157.10, 144.23, 132.83, 132.37, 129.25, 128.40, 115.22, 115.15, 110.29, 67.53, 50.51, 45.69, 42.59, 39.36, 38.65, 36.92, 32.58, 29.30, 29.20, 28.49, 24.22.

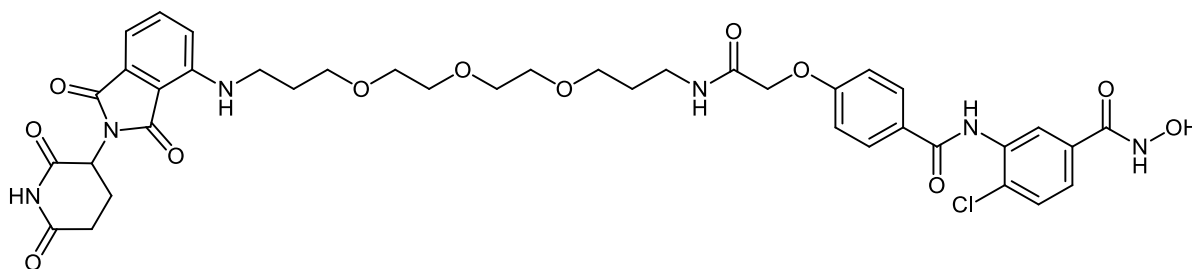
HRMS m/z: 611.300 [M+H]<sup>+</sup>, calculated C<sub>33</sub>H<sub>44</sub>ClN<sub>4</sub>O<sub>5</sub><sup>+</sup>: 611.300

HPLC: (M2) rt. 11 min (purity 98 %)

Benzyl 2-(4-(((2-chloro-5-(((tetrahydro-2*H*-pyran-2-yl)oxy)carbamoyl) phenyl) amino) methyl) phenoxy) acetate (**19**) was synthesized as shown in **scheme S1.2** in Supp. Info. Afterwards the benzyl protecting group was removed according to method VII to

yield the 2-tetrahydropyranyl protected HDAC ligand (**20**), which was reacted with E3 ligase-linker-NH<sub>2</sub> conjugates (**53**, **56**, **59**) or HyT-linker-NH<sub>2</sub> (**57**) via method IIIA. Finally, the protected PROTACs were deprotected using method V to yield PROTACs (**1g**, **1h**, **1l** and **1p**) shown in **scheme 5**.

**4-Chloro-3-(4-[(16-[[2-(2,6-dioxopiperidin-3-yl)-1,3-dioxoisindolin-4-yl]amino]-2-oxo-7,10,13-trioxa-3-azahexadecyl)oxy]benzamido)-N-hydroxybenzamide (1i)**



MS m/z: 821.47 [M-H]<sup>-</sup>

<sup>1</sup>H NMR (400 MHz, DMSO-d<sub>6</sub>) δ 11.28 (s, 1H), 11.05 (s, 1H), 9.99 (s, 1H), 9.11 (s, 1H), 8.09 (t, J = 5.6 Hz, 1H), 7.99 – 7.93 (m, 3H), 7.66 – 7.49 (m, 3H), 7.13 – 6.96 (m, 4H), 6.64 (t, J = 5.8 Hz, 1H), 5.02 (dd, J = 12.8, 5.4 Hz, 1H), 4.55 (s, 2H), 3.57 – 3.29 (m, 14H), 3.17 (dd, J = 12.8, 6.7 Hz, 2H), 2.92 – 2.79 (m, 1H), 2.61 – 2.49 (m, 2H), 2.05 – 1.95 (m, 1H), 1.83 – 1.73 (m, 2H), 1.69 – 1.59 (m, 2H).

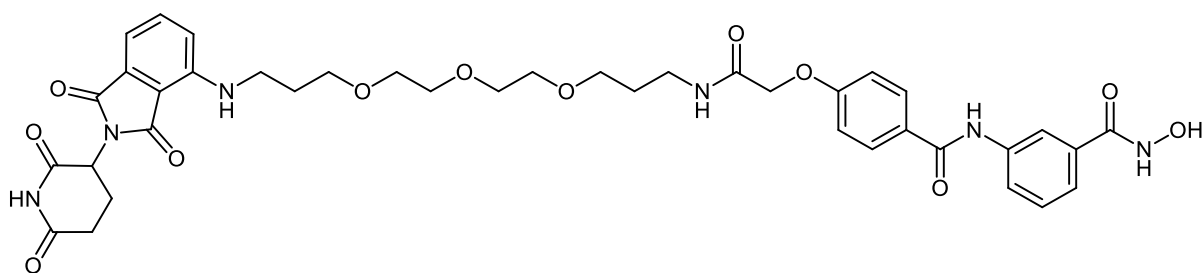
<sup>13</sup>C NMR (101 MHz, DMSO-d<sub>6</sub>) δ 173.22, 170.50, 169.29, 167.76, 167.51, 165.21, 161.05, 146.89, 136.70, 135.82, 132.63, 132.40, 130.04, 127.38, 126.40, 125.80, 117.53, 114.95, 110.82, 109.52, 70.24, 70.18, 70.14, 70.01, 68.63, 67.47, 48.98, 36.33, 31.42, 29.71, 29.33, 22.61.

HRMS m/z: 823.271 [M+H]<sup>+</sup>, calculated C<sub>39</sub>H<sub>44</sub>ClN<sub>6</sub>O<sub>12</sub><sup>+</sup>: 823.271

HPLC: (M2) rt. 9.1 min (purity 99%)

The two starting materials 4-(2-methoxy-2-oxoethoxy)benzoic acid (**21**) [68] and benzyl 3-amino-4-chlorobenzoate (**22**) which were prepared as previously described [69], were reacted together using method IIIC to afford benzyl 4-chloro-3-[4-(2-methoxy-2-oxoethoxy)benzamido]benzoate (**23**). Deprotection of the benzyl ester was achieved using method V, and the resulted acid was reacted with *O*-benzylhydroxylamine hydrochloride using method IIIA to afford methyl 2-[4-({5-[(benzyloxy)carbamoyl]-2-chlorophenyl}carbamoyl)phenoxy]acetate (**25**). The ester was then hydrolyzed using method IIB to afford the benzyl protected HDAC ligand 2-[4-({5-[(benzyloxy)carbamoyl]-2-chlorophenyl}carbamoyl)phenoxy]acetic acid (**26**). Finally, the protected HDAC ligand was reacted with E3 ligase-linker-NH<sub>2</sub> conjugate (**53**) following method IIIA to yield the protected PROTAC which was deprotected to yield PROTAC (**1i**) using method VII. **Scheme 6** illustrates the synthesis of the prescribed compound.

**3-{4-[(16-{[2-(2,6-Dioxopiperidin-3-yl)-1,3-dioxoisindolin-4-yl]amino}-2-oxo-7,10,13-trioxa-3-azahexadecyl)oxy]benzamido}-*N*-hydroxybenzamide (1j)**



MS m/z: 787.37 [M-H]<sup>-</sup>

<sup>1</sup>H NMR (400 MHz, DMSO-d<sup>6</sup>) δ 11.16 (s, 1H), 11.06 (s, 1H), 10.21 (s, 1H), 8.99 (s, 1H), 8.16 (s, 1H), 8.09 (t, *J* = 5.5 Hz, 1H), 7.99 – 7.89 (m, 3H), 7.59 – 7.51 (m, 1H), 7.44 – 7.33 (m, 2H), 7.10 – 7.04 (m, 3H), 7.00 (d, *J* = 7.1 Hz, 1H), 6.64 (t, *J* = 5.7 Hz, 1H), 5.02 (dd, *J* = 12.8, 5.5 Hz, 1H), 4.55 (s, 2H), 3.56 – 3.29 (m, 14H), 3.19 – 3.13

(m, 2H), 2.86 – 2.78 (m, 1H), 2.67 – 2.50 (m, 2H), 2.05 – 1.93 (m, 1H), 1.83 – 1.74 (m, 2H), 1.68 – 1.59 (m, 2H).

HRMS m/z: 789.310 [M+H]<sup>+</sup>, calculated C<sub>39</sub>H<sub>45</sub>N<sub>6</sub>O<sub>12</sub><sup>+</sup>: 789.310

HPLC: (M2) rt 8.7 min (purity 100%)

As illustrated in **scheme 6**, the use of 10% Pd/C in the catalytic hydrogenation to deprotect compound (**26**) resulted in the loss of the chlor in the final PROTAC (**1j**). That is the reason why a lower concentration of the catalyst was used. This led to the successful removal of the benzyl group while retaining the chlor atom.

### **Conflict of interest**

None

### **Funding**

This work was funded by the Deutsche Forschungsgemeinschaft (DFG) Si868/13-1, project number 260315923, Si868/22-1, project number 46995445 (to W.S.), Ju295/13-1, project number 260315923, to (M.J.), Oe542/2-1, project number 260315923 to (I.O.). S.D. acknowledges the funding by a full scholarship from the Ministry of Higher Education of the Arab Republic of Egypt.

### **Author Contributions**

S.D and E.G synthesized some of the compounds and wrote parts of the manuscript. T. H. synthesized some of the compounds. D.H., K.S. and P.Z. carried out the HDAC in vitro testing and analyzed data. D.R. did the docking and modelling studies. F.E. carried out the cytotoxicity testing on human HEK293 cells. J.R. performed experiments on neuroblastoma cells, C.R. expressed and provided HDAC8 protein



for in vitro testing. M.S. carried out non-enzymatic stability test. M.J., I.O., and W.S. designed experiments, analyzed data, and wrote the paper. All authors have given approval to the final version of the manuscript.

### **Supporting Information**

This material is available free of charge. The Supporting Information is available free of charge on

### **Author Information**

Corresponding Author

\*Phone: +493455525040. E-mail: [wolfgang.sippl@pharmazie.uni-halle.de](mailto:wolfgang.sippl@pharmazie.uni-halle.de)

ORCID

Manfred Jung: 0000-0002-6361-7716

Ina Oehme: 0000-0002-0827-2356

Wolfgang Sippl: 0000-0002-5985-9261

## References

1. Dupont C, Armant DR, Brenner CA (2009) Epigenetics: definition, mechanisms and clinical perspective. *Semin Reprod Med* 27 (5):351-357. doi:10.1055/s-0029-1237423
2. Beyer JN, Raniszewski NR, Burslem GM (2021) Advances and Opportunities in Epigenetic Chemical Biology. *ChemBioChem* 22 (1):17-42. doi:<https://doi.org/10.1002/cbic.202000459>
3. Arrowsmith CH, Bountra C, Fish PV, Lee K, Schapira M (2012) Epigenetic protein families: a new frontier for drug discovery. *Nature Reviews Drug Discovery* 11 (5):384-400. doi:10.1038/nrd3674
4. Dawson Mark A, Kouzarides T (2012) Cancer Epigenetics: From Mechanism to Therapy. *Cell* 150 (1):12-27. doi:<https://doi.org/10.1016/j.cell.2012.06.013>
5. Suvà ML, Riggi N, Bernstein BE (2013) Epigenetic reprogramming in cancer. *Science (New York, NY)* 339 (6127):1567-1570. doi:10.1126/science.1230184
6. Wolfson NA, Pitcairn CA, Fierke CA (2013) HDAC8 substrates: Histones and beyond. *Biopolymers* 99 (2):112-126. doi:<https://doi.org/10.1002/bip.22135>
7. Chen K, Zhang X, Wu YD, Wiest O (2014) Inhibition and mechanism of HDAC8 revisited. *J Am Chem Soc* 136 (33):11636-11643. doi:10.1021/ja501548p
8. Li W, Sun Z (2019) Mechanism of Action for HDAC Inhibitors—Insights from Omics Approaches. *Int J Mol Sci* 20 (7):1616
9. Madsen AS, Olsen CA (2012) Profiling of substrates for zinc-dependent lysine deacetylase enzymes: HDAC3 exhibits decrotonylase activity in vitro. *Angew Chem Int Ed Engl* 51 (36):9083-9087. doi:10.1002/anie.201203754
10. Du J, Zhou Y, Su X, Yu JJ, Khan S, Jiang H, Kim J, Woo J, Kim JH, Choi BH, He B, Chen W, Zhang S, Cerione RA, Auwerx J, Hao Q, Lin H (2011) Sirt5 is a NAD-dependent protein lysine demalonylase and desuccinylase. *Science* 334 (6057):806-809. doi:10.1126/science.1207861
11. Chakrabarti A, Melesina J, Kolbinger FR, Oehme I, Senger J, Witt O, Sippl W, Jung M (2016) Targeting histone deacetylase 8 as a therapeutic approach to cancer and neurodegenerative diseases. *Future Med Chem* 8 (13):1609-1634. doi:10.4155/fmc-2016-0117
12. Adhikari N, Amin SA, Jha T (2018) Selective and nonselective HDAC8 inhibitors: a therapeutic patent review. *Pharm Pat Anal* 7 (6):259-276. doi:10.4155/ppa-2018-0019
13. Amin SA, Adhikari N, Jha T (2017) Structure-activity relationships of hydroxamate-based histone deacetylase-8 inhibitors: reality behind anticancer drug discovery. *Future Med Chem* 9 (18):2211-2237. doi:10.4155/fmc-2017-0130
14. Balasubramanian S, Ramos J, Luo W, Sirisawad M, Verner E, Buggy JJ (2008) A novel histone deacetylase 8 (HDAC8)-specific inhibitor PCI-34051 induces apoptosis in T-cell lymphomas. *Leukemia* 22 (5):1026-1034. doi:10.1038/leu.2008.9
15. Oehme I, Deubzer HE, Lodrini M, Milde T, Witt O (2009) Targeting of HDAC8 and investigational inhibitors in neuroblastoma. *Expert Opinion on Investigational Drugs* 18 (11):1605-1617. doi:10.1517/14728220903241658
16. Song S, Wang Y, Xu P, Yang R, Ma Z, Liang S, Zhang G (2015) The inhibition of histone deacetylase 8 suppresses proliferation and inhibits apoptosis in gastric adenocarcinoma. *Int J Oncol* 47 (5):1819-1828. doi:10.3892/ijo.2015.3182
17. Wu J, Du C, Lv Z, Ding C, Cheng J, Xie H, Zhou L, Zheng S (2013) The up-regulation of histone deacetylase 8 promotes proliferation and inhibits apoptosis in hepatocellular carcinoma. *Dig Dis Sci* 58 (12):3545-3553. doi:10.1007/s10620-013-2867-7
18. Matthay KK, Maris JM, Schleiermacher G, Nakagawara A, Mackall CL, Diller L, Weiss WA (2016) Neuroblastoma. *Nature Reviews Disease Primers* 2 (1):16078. doi:10.1038/nrdp.2016.78
19. Phimmachanh M, Han JZR, O'Donnell YEI, Latham SL, Croucher DR (2020) Histone Deacetylases and Histone Deacetylase Inhibitors in Neuroblastoma. *Frontiers in Cell and Developmental Biology* 8 (1093). doi:10.3389/fcell.2020.578770
20. Oehme I, Deubzer HE, Wegener D, Pickert D, Linke JP, Hero B, Kopp-Schneider A, Westermann F, Ulrich SM, von Deimling A, Fischer M, Witt O (2009) Histone deacetylase 8 in neuroblastoma tumorigenesis. *Clin Cancer Res* 15 (1):91-99. doi:10.1158/1078-0432.Ccr-08-0684

21. Rettig I, Koeneke E, Trippel F, Mueller WC, Burhenne J, Kopp-Schneider A, Fabian J, Schober A, Fernekorn U, von Deimling A, Deubzer HE, Milde T, Witt O, Oehme I (2015) Selective inhibition of HDAC8 decreases neuroblastoma growth in vitro and in vivo and enhances retinoic acid-mediated differentiation. *Cell Death Dis* 6 (2):e1657-e1657. doi:10.1038/cddis.2015.24
22. Krennhrubec K, Marshall BL, Hedglin M, Verdin E, Ulrich SM (2007) Design and evaluation of 'Linkerless' hydroxamic acids as selective HDAC8 inhibitors. *Bioorg Med Chem Lett* 17 (10):2874-2878. doi:10.1016/j.bmcl.2007.02.064
23. Suzuki T, Ota Y, Ri M, Bando M, Gotoh A, Itoh Y, Tsumoto H, Tatum PR, Mizukami T, Nakagawa H, Iida S, Ueda R, Shirahige K, Miyata N (2012) Rapid discovery of highly potent and selective inhibitors of histone deacetylase 8 using click chemistry to generate candidate libraries. *J Med Chem* 55 (22):9562-9575. doi:10.1021/jm300837y
24. Suzuki T, Muto N, Bando M, Itoh Y, Masaki A, Ri M, Ota Y, Nakagawa H, Iida S, Shirahige K, Miyata N (2014) Design, synthesis, and biological activity of NCC149 derivatives as histone deacetylase 8-selective inhibitors. *ChemMedChem* 9 (3):657-664. doi:10.1002/cmdc.201300414
25. Huang WJ, Wang YC, Chao SW, Yang CY, Chen LC, Lin MH, Hou WC, Chen MY, Lee TL, Yang P, Chang CI (2012) Synthesis and biological evaluation of ortho-aryl N-hydroxycinnamides as potent histone deacetylase (HDAC) 8 isoform-selective inhibitors. *ChemMedChem* 7 (10):1815-1824. doi:10.1002/cmdc.201200300
26. Tang W, Luo T, Greenberg EF, Bradner JE, Schreiber SL (2011) Discovery of histone deacetylase 8 selective inhibitors. *Bioorg Med Chem Lett* 21 (9):2601-2605. doi:10.1016/j.bmcl.2011.01.134
27. Ingham OJ, Paranal RM, Smith WB, Escobar RA, Yueh H, Snyder T, Porco JA, Jr., Bradner JE, Beeler AB (2016) Development of a Potent and Selective HDAC8 Inhibitor. *ACS Med Chem Lett* 7 (10):929-932. doi:10.1021/acsmchemlett.6b00239
28. Zhao G, Wang G, Bai H, Li T, Gong F, Yang H, Wen J, Wang W (2017) Targeted inhibition of HDAC8 increases the doxorubicin sensitivity of neuroblastoma cells via up regulation of miR-137. *Eur J Pharmacol* 802:20-26. doi:10.1016/j.ejphar.2017.02.035
29. Whitehead L, Dobler MR, Radetich B, Zhu Y, Atadja PW, Claiborne T, Grob JE, McRiner A, Pancost MR, Patnaik A, Shao W, Shultz M, Tichkule R, Tommasi RA, Vash B, Wang P, Stams T (2011) Human HDAC isoform selectivity achieved via exploitation of the acetate release channel with structurally unique small molecule inhibitors. *Bioorg Med Chem* 19 (15):4626-4634. doi:10.1016/j.bmc.2011.06.030
30. Heimbürg T, Kolbinger FR, Zeyen P, Ghazy E, Herp D, Schmidtkunz K, Melesina J, Shaik TB, Erdmann F, Schmidt M, Romier C, Robaa D, Witt O, Oehme I, Jung M, Sippl W (2017) Structure-Based Design and Biological Characterization of Selective Histone Deacetylase 8 (HDAC8) Inhibitors with Anti-Neuroblastoma Activity. *J Med Chem* 60 (24):10188-10204. doi:10.1021/acs.jmedchem.7b01447
31. Itoh Y (2018) Chemical Protein Degradation Approach and its Application to Epigenetic Targets. *The Chemical Record* 18 (12):1681-1700. doi:<https://doi.org/10.1002/tcr.201800032>
32. Lai AC, Crews CM (2017) Induced protein degradation: an emerging drug discovery paradigm. *Nature Reviews Drug Discovery* 16 (2):101-114. doi:10.1038/nrd.2016.211
33. Cromm PM, Crews CM (2017) Targeted Protein Degradation: from Chemical Biology to Drug Discovery. *Cell Chemical Biology* 24 (9):1181-1190. doi:<https://doi.org/10.1016/j.chembiol.2017.05.024>
34. Wang Y, Jiang X, Feng F, Liu W, Sun H (2020) Degradation of proteins by PROTACs and other strategies. *Acta Pharmaceutica Sinica B* 10 (2):207-238. doi:<https://doi.org/10.1016/j.apsb.2019.08.001>
35. Sakamoto KM, Kim KB, Kumagai A, Mercurio F, Crews CM, Deshaies RJ (2001) Protacs: chimeric molecules that target proteins to the Skp1-Cullin-F box complex for ubiquitination and degradation. *Proc Natl Acad Sci U S A* 98 (15):8554-8559. doi:10.1073/pnas.141230798
36. Pettersson M, Crews CM (2019) PROteolysis TARgeting Chimeras (PROTACs) — Past, present and future. *Drug Discovery Today: Technologies* 31:15-27. doi:<https://doi.org/10.1016/j.ddtec.2019.01.002>
37. Smalley JP, Cowley SM, Hodgkinson JT (2020) Bifunctional HDAC Therapeutics: One Drug to Rule Them All? *Molecules* 25 (19):4394

38. Gadd MS, Testa A, Lucas X, Chan KH, Chen W, Lamont DJ, Zengerle M, Ciulli A (2017) Structural basis of PROTAC cooperative recognition for selective protein degradation. *Nat Chem Biol* 13 (5):514-521. doi:10.1038/nchembio.2329
39. Schiedel M, Herp D, Hammelmann S, Swyter S, Lehotzky A, Robaa D, Oláh J, Ovádi J, Sippl W, Jung M (2018) Chemically Induced Degradation of Sirtuin 2 (Sirt2) by a Proteolysis Targeting Chimera (PROTAC) Based on Sirtuin Rearranging Ligands (SirReals). *J Med Chem* 61 (2):482-491. doi:10.1021/acs.jmedchem.6b01872
40. Yang K, Song Y, Xie H, Wu H, Wu Y-T, Leisten ED, Tang W (2018) Development of the first small molecule histone deacetylase 6 (HDAC6) degraders. *Bioorg Med Chem Lett* 28 (14):2493-2497. doi:<https://doi.org/10.1016/j.bmcl.2018.05.057>
41. Liu J-R, Yu C-W, Hung P-Y, Hsin L-W, Chern J-W (2019) High-selective HDAC6 inhibitor promotes HDAC6 degradation following autophagy modulation and enhanced antitumor immunity in glioblastoma. *Biochem Pharmacol* 163:458-471. doi:<https://doi.org/10.1016/j.bcp.2019.03.023>
42. Yang K, Wu H, Zhang Z, Leisten ED, Nie X, Liu B, Wen Z, Zhang J, Cunningham MD, Tang W (2020) Development of Selective Histone Deacetylase 6 (HDAC6) Degraders Recruiting Von Hippel–Lindau (VHL) E3 Ubiquitin Ligase. *ACS Med Chem Lett* 11 (4):575-581. doi:10.1021/acsmedchemlett.0c00046
43. Wu H, Yang K, Zhang Z, Leisten ED, Li Z, Xie H, Liu J, Smith KA, Novakova Z, Barinka C, Tang W (2019) Development of Multifunctional Histone Deacetylase 6 Degraders with Potent Antimyeloma Activity. *J Med Chem* 62 (15):7042-7057. doi:10.1021/acs.jmedchem.9b00516
44. Smalley JP, Adams GE, Millard CJ, Song Y, Norris JKS, Schwabe JWR, Cowley SM, Hodgkinson JT (2020) PROTAC-mediated degradation of class I histone deacetylase enzymes in corepressor complexes. *Chem Commun* 56 (32):4476-4479. doi:10.1039/D0CC01485K
45. Roatsch MV, Anja; Herp, Daniel; Jung, Manfred; Olsen, Christian Adam (2020) Proteolysis-Targeting Chimeras (PROTACs) Based on Macrocyclic Tetrapeptides Selectively Degrade Class I Histone Deacetylases 1–3. . ChemRxiv. doi: doi: 10.26434/chemrxiv.12416303.v1
46. Xiao Y, Wang J, Zhao LY, Chen X, Zheng G, Zhang X, Liao D (2020) Discovery of histone deacetylase 3 (HDAC3)-specific PROTACs. *Chem Commun* 56 (68):9866-9869. doi:10.1039/D0CC03243C
47. Xiong Y, Donovan KA, Eleuteri NA, Kirmani N, Yue H, Razov A, Krupnick NM, Nowak RP, Fischer ES (2021) Chemo-proteomics exploration of HDAC degradability by small molecule degraders. *Cell Chemical Biology* 28 (10):1514-1527.e1514. doi:<https://doi.org/10.1016/j.chembiol.2021.07.002>
48. Heimbürg T, Chakrabarti A, Lancelot J, Marek M, Melesina J, Hauser A-T, Shaik TB, Duclaud S, Robaa D, Erdmann F, Schmidt M, Romier C, Pierce RJ, Jung M, Sippl W (2016) Structure-Based Design and Synthesis of Novel Inhibitors Targeting HDAC8 from *Schistosoma mansoni* for the Treatment of Schistosomiasis. *J Med Chem* 59 (6):2423-2435. doi:10.1021/acs.jmedchem.5b01478
49. Marek M, Shaik TB, Heimbürg T, Chakrabarti A, Lancelot J, Ramos-Morales E, Da Veiga C, Kalinin D, Melesina J, Robaa D, Schmidtkunz K, Suzuki T, Holl R, Ennifar E, Pierce RJ, Jung M, Sippl W, Romier C (2018) Characterization of Histone Deacetylase 8 (HDAC8) Selective Inhibition Reveals Specific Active Site Structural and Functional Determinants. *J Med Chem* 61 (22):10000-10016. doi:10.1021/acs.jmedchem.8b01087
50. Lai AC, Toure M, Hellerschmied D, Salami J, Jaime-Figueroa S, Ko E, Hines J, Crews CM (2016) Modular PROTAC Design for the Degradation of Oncogenic BCR-ABL. *Angew Chem Int Ed* 55 (2):807-810. doi:<https://doi.org/10.1002/anie.201507634>
51. Smith BE, Wang SL, Jaime-Figueroa S, Harbin A, Wang J, Hamman BD, Crews CM (2019) Differential PROTAC substrate specificity dictated by orientation of recruited E3 ligase. *Nat Commun* 10 (1):131. doi:10.1038/s41467-018-08027-7
52. Cyrus K, Wehenkel M, Choi EY, Han HJ, Lee H, Swanson H, Kim KB (2011) Impact of linker length on the activity of PROTACs. *Mol Biosyst* 7 (2):359-364. doi:10.1039/c0mb00074d
53. Zorba A, Nguyen C, Xu Y, Starr J, Borzilleri K, Smith J, Zhu H, Farley KA, Ding W, Schiemer J, Feng X, Chang JS, Uccello DP, Young JA, Garcia-Irrizary CN, Czabaniuk L, Schuff B, Oliver R, Montgomery J, Hayward MM, Coe J, Chen J, Niosi M, Luthra S, Shah JC, El-Kattan A, Qiu X, West GM, Noe MC, Shanmugasundaram V, Gilbert AM, Brown MF, Calabrese MF (2018) Delineating the role of cooperativity in the design of potent PROTACs for BTK. *Proc Natl Acad Sci U S A* 115 (31):E7285-e7292. doi:10.1073/pnas.1803662115

54. Nowak RP, DeAngelo SL, Buckley D, He Z, Donovan KA, An J, Safaee N, Jedrychowski MP, Ponthier CM, Ishoey M, Zhang T, Mancias JD, Gray NS, Bradner JE, Fischer ES (2018) Plasticity in binding confers selectivity in ligand-induced protein degradation. *Nat Chem Biol* 14 (7):706-714. doi:10.1038/s41589-018-0055-y
55. Cyrus K, Wehenkel M, Choi E-Y, Lee H, Swanson H, Kim K-B (2010) Jostling for Position: Optimizing Linker Location in the Design of Estrogen Receptor-Targeting PROTACs. *ChemMedChem* 5 (7):979-985. doi:<https://doi.org/10.1002/cmdc.201000146>
56. Zoppi V, Hughes SJ, Maniaci C, Testa A, Gmaschitz T, Wieshofer C, Koegl M, Riching KM, Daniels DL, Spallarossa A, Ciulli A (2019) Iterative Design and Optimization of Initially Inactive Proteolysis Targeting Chimeras (PROTACs) Identify VZ185 as a Potent, Fast, and Selective von Hippel–Lindau (VHL) Based Dual Degradation Probe of BRD9 and BRD7. *J Med Chem* 62 (2):699-726. doi:10.1021/acs.jmedchem.8b01413
57. Goracci L, Desantis J, Valeri A, Castellani B, Eleuteri M, Cruciani G (2020) Understanding the Metabolism of Proteolysis Targeting Chimeras (PROTACs): The Next Step toward Pharmaceutical Applications. *J Med Chem* 63 (20):11615-11638. doi:10.1021/acs.jmedchem.0c00793
58. Bricelj A, Dora Ng YL, Ferber D, Kuchta R, Müller S, Monschke M, Wagner KG, Krönke J, Sosič I, Gütschow M, Steinebach C (2021) Influence of Linker Attachment Points on the Stability and Neosubstrate Degradation of Cereblon Ligands. *ACS Med Chem Lett* 12 (11):1733-1738. doi:10.1021/acsmchemlett.1c00368
59. Hu Z, Crews CM (2022) Recent Developments in PROTAC-Mediated Protein Degradation: From Bench to Clinic. *ChemBioChem* 23 (2):e202100270. doi:<https://doi.org/10.1002/cbic.202100270>
60. Klein VG, Bond AG, Craigon C, Lokey RS, Ciulli A (2021) Amide-to-Ester Substitution as a Strategy for Optimizing PROTAC Permeability and Cellular Activity. *J Med Chem* 64 (24):18082-18101. doi:10.1021/acs.jmedchem.1c01496
61. Lepper ER, Smith NF, Cox MC, Scripture CD, Figg WD (2006) Thalidomide metabolism and hydrolysis: mechanisms and implications. *Curr Drug Metab* 7 (6):677-685. doi:10.2174/138920006778017777
62. Darwish S, Heimburg T, Ridinger J, Herp D, Schmidt M, Romier C, Jung M, Oehme I, Sippl W (in press) Synthesis, Biochemical and Cellular Evaluation of HDAC6 targeting proteolysis targeting chimeras. In: *Methods in Molecular Biology, HDAC/HAT Function Assessment and Inhibitor Development: Methods and Protocols*, Second Edition edn. Springer Nature,
63. Ghazy E, Zeyen P, Herp D, Hügler M, Schmidtkunz K, Erdmann F, Robaa D, Schmidt M, Morales ER, Romier C, Günther S, Jung M, Sippl W (2020) Design, synthesis, and biological evaluation of dual targeting inhibitors of histone deacetylase 6/8 and bromodomain BRPF1. *Eur J Med Chem* 200:112338. doi:<https://doi.org/10.1016/j.ejmech.2020.112338>
64. Stolfa DA, Stefanachi A, Gajer JM, Nebbioso A, Altucci L, Cellamare S, Jung M, Carotti A (2012) Design, Synthesis, and Biological Evaluation of 2-Aminobenzanilide Derivatives as Potent and Selective HDAC Inhibitors. *ChemMedChem* 7 (7):1256-1266. doi:<https://doi.org/10.1002/cmdc.201200193>
65. Marek M, Kannan S, Hauser A-T, Moraes Mourão M, Caby S, Cura V, Stolfa DA, Schmidtkunz K, Lancelot J, Andrade L, Renaud J-P, Oliveira G, Sippl W, Jung M, Cavarelli J, Pierce RJ, Romier C (2013) Structural Basis for the Inhibition of Histone Deacetylase 8 (HDAC8), a Key Epigenetic Player in the Blood Fluke *Schistosoma mansoni*. *PLOS Pathogens* 9 (9):e1003645. doi:10.1371/journal.ppat.1003645
66. Samadi S, Jadidi K, Khanmohammadi B, Tavakoli N (2016) Heterogenization of chiral mono oxazoline ligands by grafting onto mesoporous silica MCM-41 and their application in copper-catalyzed asymmetric allylic oxidation of cyclic olefins. *J Catal* 340:344-353. doi:<https://doi.org/10.1016/j.jcat.2016.05.021>
67. Nagaoka Y, Maeda T, Kawai Y, Nakashima D, Oikawa T, Shimoke K, Ikeuchi T, Kuwajima H, Uesato S (2006) Synthesis and cancer antiproliferative activity of new histone deacetylase inhibitors: hydrophilic hydroxamates and 2-aminobenzamide-containing derivatives. *Eur J Med Chem* 41 (6):697-708. doi:<https://doi.org/10.1016/j.ejmech.2006.02.002>

68. Tang W, Luo T, Greenberg EF, Bradner JE, Schreiber SL (2011) Discovery of histone deacetylase 8 selective inhibitors. *Bioorg Med Chem Lett* 21 (9):2601-2605.

doi:<https://doi.org/10.1016/j.bmcl.2011.01.134>

69. Kubik S, Goddard R (2001) Fine tuning of the cation affinity of artificial receptors based on cyclic peptides by intramolecular conformational control. *European Journal of Organic Chemistry* 2001 (2):311-322. doi:10.1002/1099-0690(200101)2001:2<311::Aid-ejoc311>3.0.Co;2-m